Supporting Information for

Reticular Design and Alkyne Bridge Engineering in Donor-π-Acceptor Type Conjugated Microporous Polymers for Boosting Photocatalytic Hydrogen Evolution

Mohamed Gamal Mohamed[a,b]*, Mohamed Hammad Elsayed[c,d]*, Chia-Jung Li[a], Ahmed E. Hassan[d], Islam M. A. Mekhemer[b,c], Ahmed Fouad Musa[c], Mahmoud Kamal Hussien[e,b], Li-Chyong Chen[e,f,g], Kuei-Hsien Chen[e,h], Ho-Hsiu Chou[c], Shiao-Wei Kuo[a,i]*

[a]Department of Materials and Optoelectronic Science, Center for Functional Polymers and Supramolecular Materials, National Sun Yat-Sen University, Kaohsiung 804, Taiwan.
[b]Department of Chemistry, Faculty of Science, Assiut University, Assiut, Egypt.
[c]Department of Chemical Engineering, National Tsing Hua University, Hsinchu 30013, Taiwan.
[d]Department of Chemistry, Faculty of Science, Al-Azhar University, Nasr City, Cairo 11884, Egypt.
[e]Center for Condensed Matter Sciences, National Taiwan University, Taipei 10617, Taiwan.
[f]Center of Atomic Initiative for New Materials, National Taiwan University, Taipei 10617, Taiwan.
[g]Department of Physics, National Taiwan University, Taipei 10617, Taiwan.
[h]Institute of Atomic and Molecular Sciences, Academia Sinica, Taipei 10617, Taiwan.
[i]Department of Medicinal and Applied Chemistry, Kaohsiung Medical University, Kaohsiung 807, Taiwan.

Corresponding authors: mgaml.eldin12@yahoo.com (M. G. Mohamed), Mohamed.hammad@azhar.edu.eg (M. H. Elsayed) and kuosw@faculty.nsysu.edu.tw (S. W. Kuo).

Characterization

FTIR spectra were collected on a Bruker Tensor 27 FTIR spectrophotometer with a resolution of 4 cm^{-1} by using the KBr disk method. ^{13}C nuclear magnetic resonance (NMR) spectra were examined by using an INOVA 500 instrument with DMSO as the solvent and TMS as the external standard. Chemical shifts are reported in parts per million (ppm). The curing behavior and thermal stabilities of the samples were performed by using a TG Q-50 thermogravimetric analyzer under a N_2 atmosphere; the cured sample (ca. 5 mg) was put in a Pt cell with a heating rate of 20 °C min^{-1} from 100 to 800 °C under a N_2 flow rate of 60 mL min^{-1}. Wide-angle X-ray diffraction (WAXD) patterns were measured by the wiggler beamline BL17A1 of the National Synchrotron Radiation Research Center (NSRRC), Taiwan. A triangular bent Si (111) single crystal was used to get a monochromated beam having a wavelength (λ) of 1.33 Å. The morphologies of the polymer samples were examined by Field emission scanning electron microscopy (FE-SEM; JEOL JSM7610F) and transmission electron microscope (TEM) using a JEOL-2100 instrument at an accelerating voltage of 200 kV. Surface area and porosity measurements of samples weighing approximately 40-60 mg were conducted using the BEL MasterTM/BEL simTM (version 3.0.0) apparatus. Nitrogen (N_2) adsorption and desorption isotherms were generated by gradually exposing the samples to ultrahigh-purity N_2 gas, reaching pressures of up to about 1 atmosphere, while maintaining a temperature of 77 K in a liquid nitrogen bath. Prior to these measurements, the samples underwent a degassing process at 150 °C for a duration of 8 hours. The instrument's software was utilized to calculate surface parameters using the BET adsorption models. Furthermore, the pore size of the prepared samples was determined using nonlocal density functional theory (NLDFT).

Synthesis of 1,3,6,8-tetrabromopyrene (Py-Br_4)

Pyrene (1.00 g,5 mmol) was dissolved in nitrobenzene (10 mL) and a solution of bromine (1.15 mL, 22 mmol) with nitrobenzene (10 mL) was added dropwise into it, the mixture was heated up to 120°C for 4 h and then cooled to room temperature, the reaction mixture was filtered, washed with ETOH and dried under vacuum at 50°C to afford a green solid (2.20 g, 91%). FT-IR (KBr): 3053 (aromatic C–H stretching), 682 (C–Br stretching).

Synthesis of 1,3,6,8-tetrakis(2-(trimethylsilyl)ethynyl)pyrene (Py-TMS)

Under nitrogen, $Pd(PPh_3)_4$ (220 mg, 0.12 mmol), PPh_3 (244 mg, 0.92 mmol), and CuI (118 mg, 0.62 mmol) were added to 1,3,6,8-tetrabromopyrene (2 g, 2.38 mmol) in a mixed solvent of dry toluene (28 mL) and triethylamine (28 mL). After being heated up to 50°C, TMSA (2.34 g, 23.8 mmol) was injected dropwise into the flask, and the mixture was stirred under 90°C for 48 h, the reaction mixture was cooled to room temperature and filtered through Celite. Then, the solvent was removed under reduced pressure to give an orange solid. FT-IR (KBr, cm^{-1}): 3053 (aromatic C–H stretching), 2908 (aliphatic C–H stretching), 2100 (C≡C stretching), 1618 (C=C stretching). ^1H NMR (500 MHz, δ, ppm, $CDCl_3$): 0.413 (s, 36H, CH_3), 8.3 (s, 2H), 8.57 (s, 4H). ^{13}C NMR (125 MHz, δ, ppm, $CDCl_3$): 135.70, 132.40, 127.80, 119.20, 103.50, 101.60.

Synthesis of 1,3,6,8-tetraethynylpyrene (Py-T)

1,3,6,8-tetrakis(2-(trimethylsilyl)ethynyl)pyrene (2.00 g, 3.41 mmol) and K_2CO_3 (5.70 g, 42 mmol) were added in one neck flask with anhydrous methanol (50 mL)and the reaction mixture was stirred at room temperature for 48 h. The methanol solution was removed under reduced pressure to afford 1,3,6,8-tetraethynylpyrene as an orange powder (1.88 g, 94.30%, Scheme S1). FT-IR (KBr, cm^{-1}, **Figure S1**): 3279 (≡C-H), 3065 (aromatic C–H stretching), 2186 (C≡C stretching), 1618 (C=C

stretching).^{1}H NMR (500 MHz, δ, ppm, $CDCl_3$, **Figure S2**): 8.68 (s, 4H), 8.38 (s, 2H), 3.67 (s, 4H). ^{13}C NMR (125 MHz, δ, ppm, $CDCl_3$, **Figure S3**): 133.80, 130.80, 129.10, 127.80, 84.50, 59.70.

Synthesis of Tetraphenylethylene (TPE) and 1,1,2,2-Tetrakis(4-bromophenyl)ethene (TPE-Br_4) under N_2, benzophenone (3.00 g, 16.4 mmol) and Zn (4.31g, 65.9 mmol) in THF (80 mL) were stirred in an ice/salt-water bath for 10 min. $TiCl_4$ (3.60 mL, 33.0 mmol) was injected over 30 min, and then the mixture was kept at 80 °C under reflux. Then, 5% aqueous K_2CO_3 was added to the reaction. After evaporation of the organic solvent, EtOAc extracted the aqueous phase three times. After evaporation of EtOAc, the residue was washed with EtOH to obtain a white crystalline solid (2.66 g, 97%). M.p.: 228–229 °C (DSC). FTIR (KBr, cm^{-1}): 3047 (aromatic C–H stretching), 1602 (C=C stretching). ^{1}H NMR (500 MHz, $CDCl_3$, δ, ppm): 7.26 (d, 8H), 6.84 (d, 8H). ^{13}C NMR (125 MHz, $CDCl_3$, δ, ppm): 140.70, 141.00, 131.30, 127.70, 126.4. A solution of TPE (3.32 g, 10.0 mmol) in glacial acetic acid (10 mL) and CH_2Cl_2 (20 mL) in a round-bottom flask at 0 °C (ice bath). Br_2 (4.00 mL, 80.0 mmol) was added to the mixture, and the mixture was kept at room temperature for 48 h. Then, the H_2O (200 mL) was added to the resulting solution, and the mixture was extracted with CH_2Cl_2. After evaporation of CH_2Cl_2, the residue was washed with MeOH to give a white solid, which was recrystallized (CH_2Cl_2/MeOH) to give TPE-Br_4 a white crystalline solid (6.15 g, 95%). M.p.: 261–262 °C (DSC). FTIR (KBr, cm^{-1}): 3051 (aromatic C–H stretching), 1572 (C=C stretching). ^{1}H NMR (500 MHz, $CDCl_3$, δ, ppm): 7.25 (d, 8H), 6.84 (d, 8H). ^{13}C NMR (125 MHz, $CDCl_3$, δ, ppm): 142.30, 139.70, 133.70, 131.90, 121.80.

1,1,2,2-Tetrakis(4-((trimethylsilyl)ethynyl)phenyl)ethane (TPE-TMS)

A mixture of TPE-Br_4 (1.00 g, 1.54 mmol), CuI (0.0470 g, 0.240 mmol), PPh_3 (0.100 g, 0.380 mmol), and $Pd(PPh_3)_4$ (0.0860 g, 0.120 mmol) in THF (14 mL) and Et_3N (14 mL) was stirred in a two-neck flask at 50 °C for 30 min. Ethynyltrimethylsilane (1.21 g, 12.3 mmol) was added dropwise and then

the mixture was heated under reflux at 50 °C for 3 days. The resulting mixture was filtered and concentrated. The residue was purified through flash chromatography (SiO_2; DCM) to give a white powder (0.75 g, 75%). FTIR (KBr, cm^{-1}): 3060 (aromatic C–H stretching), 2920 (aliphatic C–H stretching), 2155 (C≡C stretching), 1618 (C=C stretching). ^{1}H NMR (500 MHz, $CDCl_3$, δ, ppm): 7.24 (d, J = 8.4 Hz, 8H), 6.88 (d, J = 8.4 Hz, 8H), 0.22 (s, 36H, CH_3). ^{13}C NMR (125 MHz, $CDCl_3$, δ, ppm): 144, 141, 132.7, 132, 122.3, 105.6, 95.8, 0.07.

1,1,2,2-Tetrakis(4-ethynylphenyl)ethene (TPE-T)

A mixture of TPE-TMS (0.440 g, 0.650 mmol) and K_2CO_3 (0.900 g, 6.52 mmol) in methanol (10 mL) was stirred at room temperature overnight. The pale-yellow precipitate [**Scheme S2**] was filtered off and dried [0.37 g, 93%: T_m: 155.5 °C (DSC)]. FTIR (KBr, cm^{-1}, **Figure S4**): 3273 (≡C–H), 3042 (aromatic C–H stretching), 2109 (C≡C stretching), 1617 (C=C stretching). ^{1}H NMR (500 MHz, $CDCl_3$, δ, ppm, **Figure S5**): 7.24 (d, J = 8.4 Hz, 8H), 6.93 (d, J = 8.4 Hz, 8H), 3.06 (s, 4H, ≡C–H). ^{13}C NMR (125 MHz, $CDCl_3$, δ, ppm, **Figure S6**): 143.8, 141.6, 132.36, 132, 121.24, 83.6 (≡C–Ar), 77.88 (≡C–H).

Photocatalytic H_2 evolution tests

Electrochemical impedance spectroscopy (EIS)

Electrochemical impedance spectroscopy (EIS) was performed on a Zahner Zennium E workstation equipped with three-electrode cells including a Pt wire counter electrode, Ag/AgCl as reference electrode (3M NaCl), and a fluorine-doped tin oxide (FTO) glass as a working electrode. About 5 mg of CMPs were dispersed into an acetonitrile solution (1 mL) with 30 μL Nafion and sonicate for 1 h. After that, 200 μL of as-prepared suspension was spin-coated on FTO glass with an active area of 6.875 cm^2. Here, 0.5 M Na_2SO_4 aqueous solution was prepared as an electrolyte.

Photocatalytic H_2 evolution test

The photocatalytic experiments were carried out in a 35 mL Pyrex reactor. The reactor was closed using a rubber septum. In a typical photocatalytic reaction, TPA-TPA CMP or TPE-TPA CMP or Py-TPA CMP or TPA-TB-TPA CMP or TPE-TB-TPA CMP or Py-TB-TPA CMP (1 mg) was dispersed in 10 mL of the mixture of water/methanol (2/1) with 0.1M AA as the sacrificial electron donor. The suspension was purged with argon for 5 min to remove dissolved air. A 350 W Xenon lamp equipped with a cut-off filter (1000 W/m^2, λ: 380-780 nm) was used as the light source. The light intensity of the Xe lamp was similar to that of the visible light region in standard 1 sun, as verified using a solar cell. Hydrogen samples were taken with a gas-tight syringe and injected in a Shimazhu GC-2014 gas chromatograph with Ar as the carrier gas. Hydrogen was detected with a thermal conductivity detector, referring to the standard hydrogen gases with known concentrations.

Quantum efficiency measurements

In the AQY experiments, the catalyst solution was prepared by dispersing Py-TB-TPA CMP (1 mg) in 10 mL of the mixture of water/methanol (2/1) with 0.1M AA as sacrificial electron donor and cocatalyst (2 wt% Pt). The suspension was illuminated with a 300 W Xe lamp with different bandpass filters (420, 460, 500, and 600 nm). The formation of hydrogen was quantified using a Shimadzu gas chromatograph (GC2014) operating at isothermal conditions using a semi-capillary column equipped with a thermal conductivity detector.

The AQY was calculated as follows:

AQY = [(Number of evolved hydrogen molecules ×2) / Number of incident photons] × 100%.

The AQY was calculated as follows:

AQY = [(Number of evolved hydrogen molecules ×2) / Number of incident photons] × 100%

$$AQY = \frac{N_e}{N_p} \times 100\% = \frac{2 \times M \times N_A}{\frac{E_{total}}{E_{photon}}} \times 100\%$$

$$= \frac{2M \times N_A}{\frac{S \times P \times t}{h \times \frac{c}{\lambda}}} \times 100\% = \frac{2 \times M \times N_A \times h \times c}{S \times P \times t \times \lambda} \times 100\%$$

Where M is the amount of H_2 molecules (mol), N_A is Avogadro constant (6.022×10^{23}/mol), h is the Planck constant (6.626×10^{-34} J·s), c is the speed of light (3×108 m/s), S is the irradiation area (cm^2), P is the intensity of irradiation light (W/cm^2), t is the photoreaction time (s), λ is the wavelength of the monochromatic light (m).

The experimental details for DFT calculations

Density functional theory (DFT) is a computational method used to calculate the electronic structure of atoms, molecules, and materials. DFT calculations can be used to predict various properties of these systems, such as their geometry, electronic properties, and vibrational frequencies. The ground state geometry optimization of the CMPs molecules is implemented using Density Functional Theory (DFT) whilst applying the methods of B3LYP at 6-31G (d) basis set method at Gaussian 16 revision A.03 program package. The obtained result was then visualized using the Gauss View 5 software.

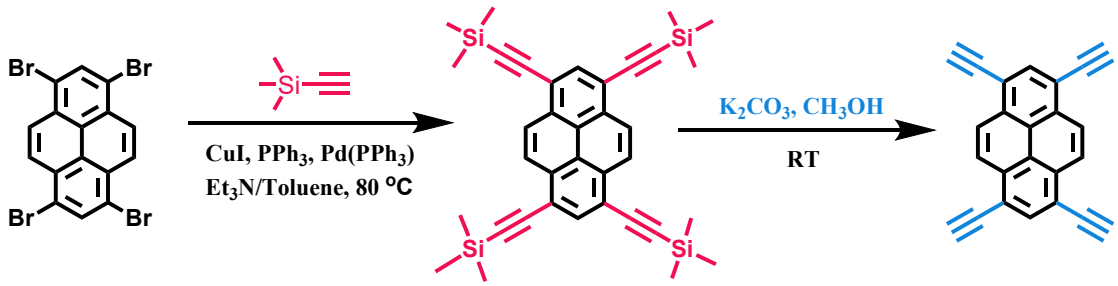

Scheme S1. Synthesis of Py-T.

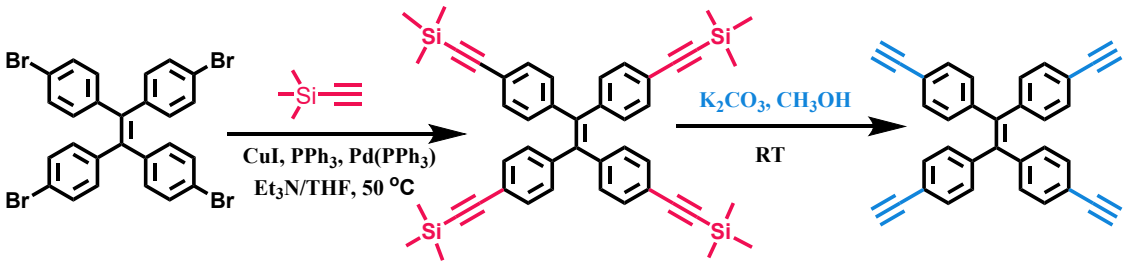

Scheme S2. Synthesis of TPE-T.

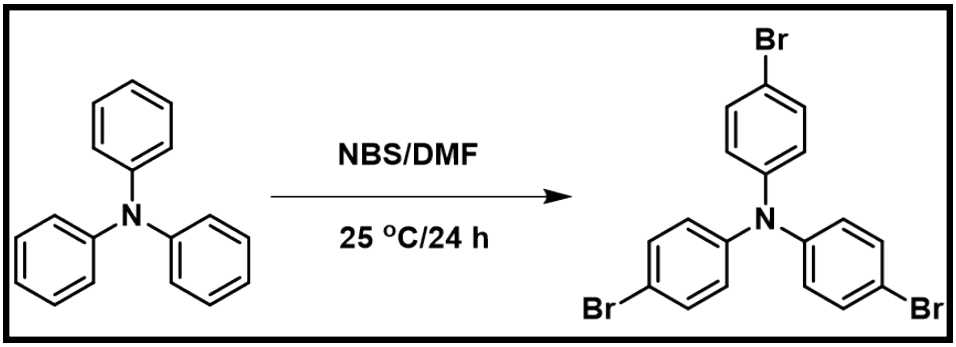

Scheme S3. Synthesis of TPA-3Br.

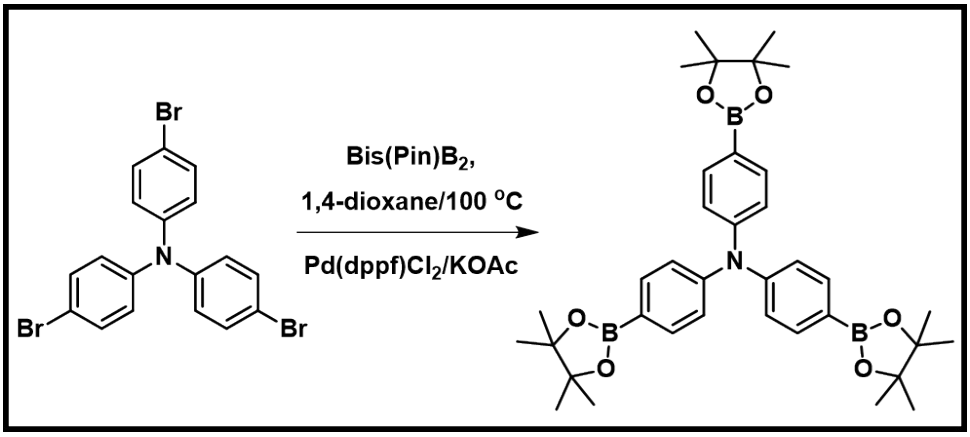

Scheme S4. Synthesis of TPA-3B(OCH_3)$_2$.

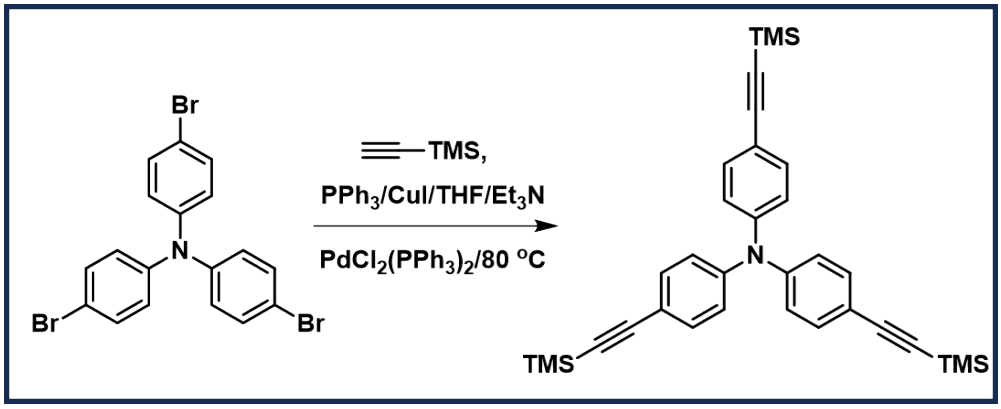

Scheme S5. Synthesis of TPA-TMS.

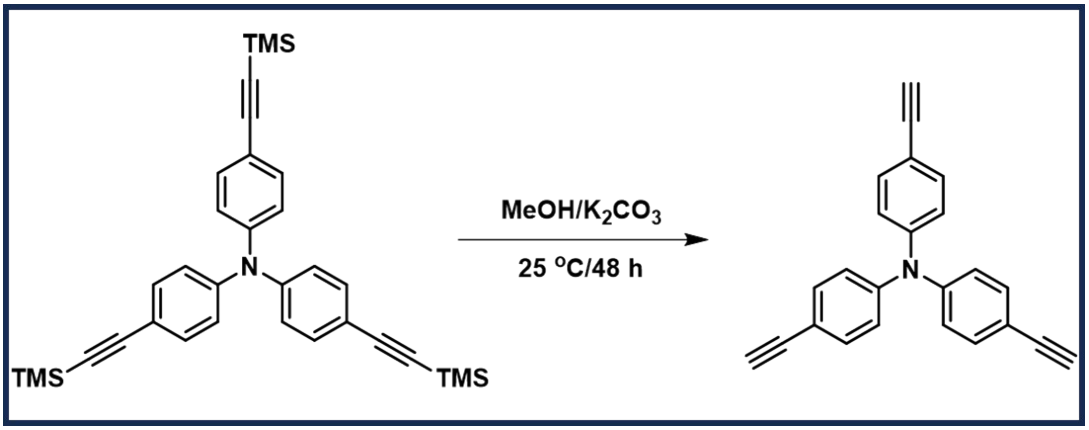

Scheme S6. Synthesis of TPA-T.

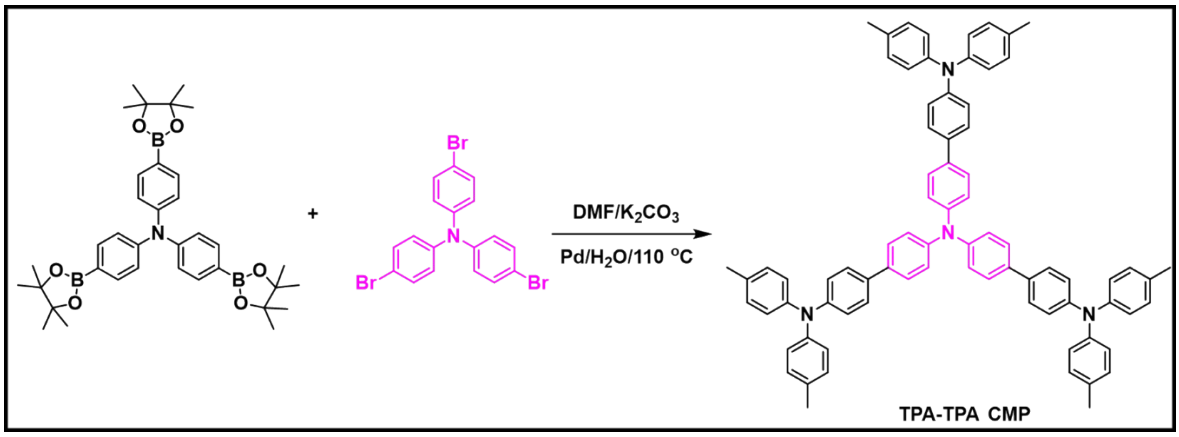

Scheme S7. Synthesis of TPA-TPA CMP.

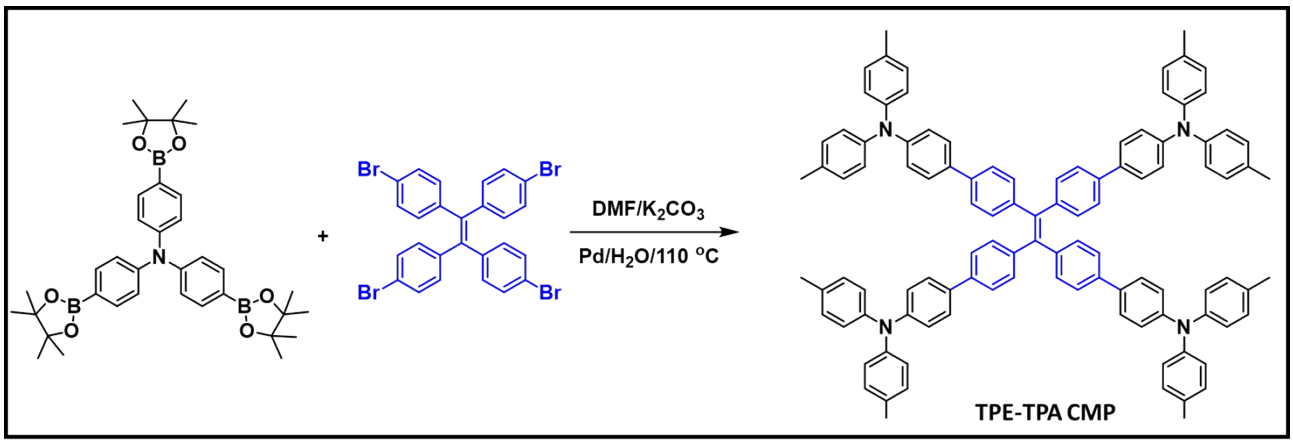

Scheme S8. Synthesis of TPE-TPA CMP.

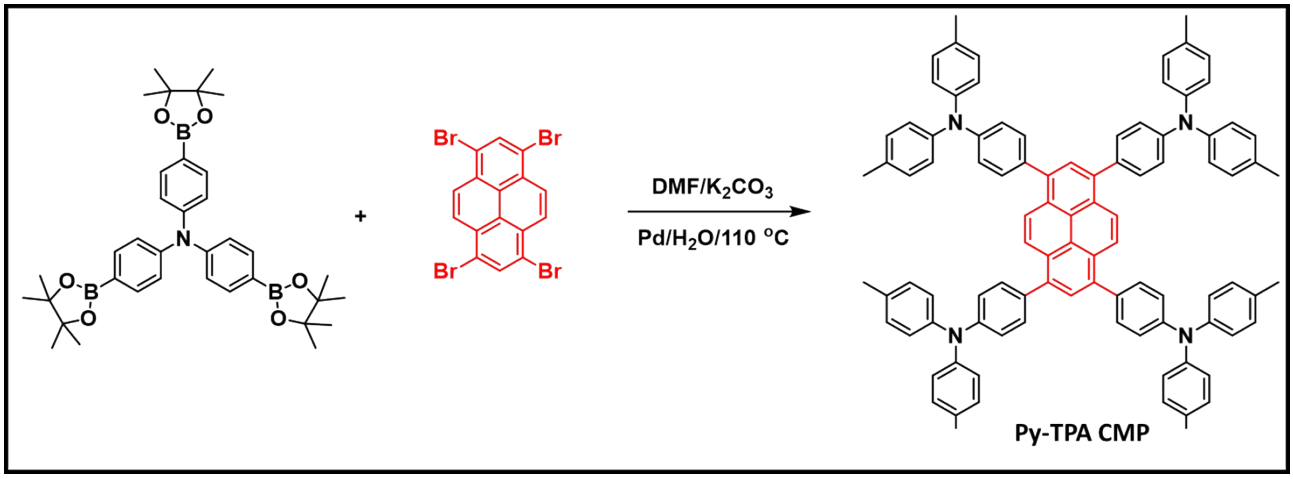

Scheme S9. Synthesis of Py-TPA CMP.

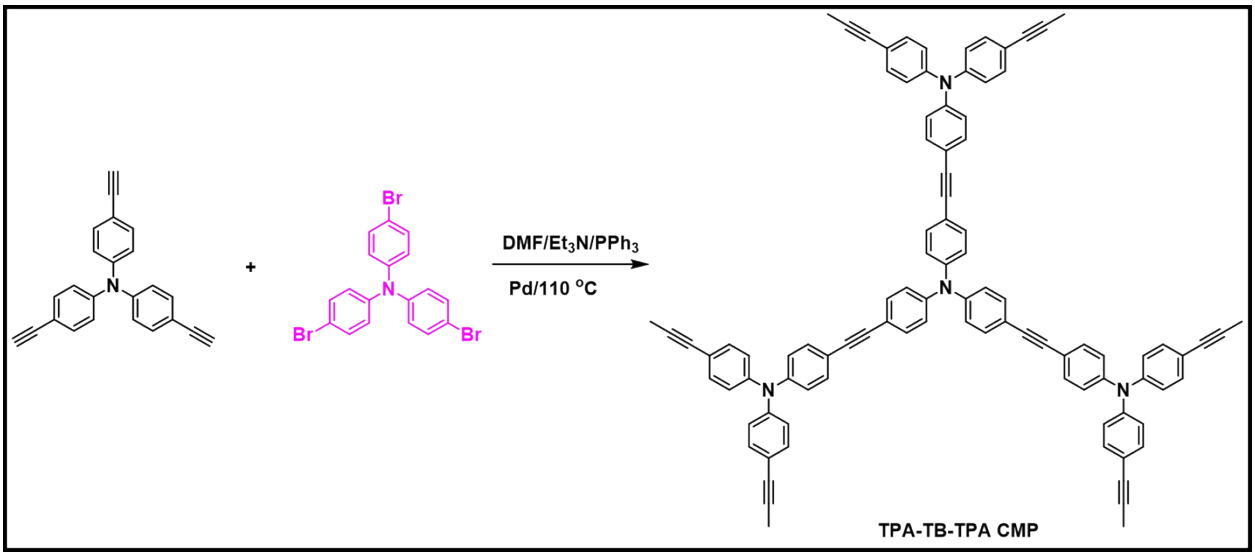

Scheme S10. Synthesis of TPA-TB-TPA CMP.

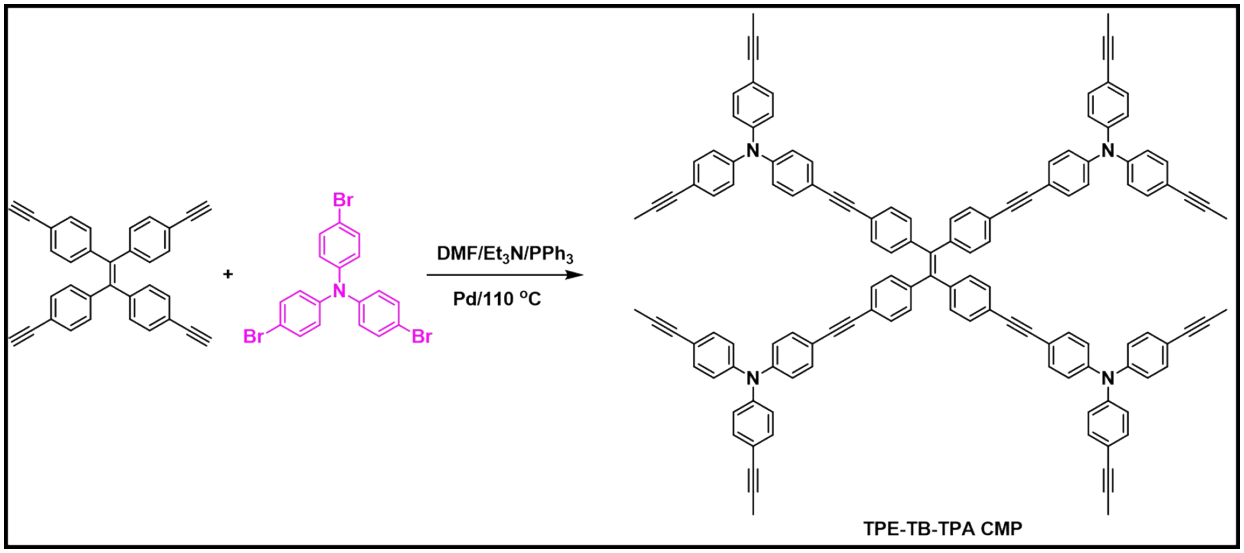

Scheme S11. Synthesis of TPE-TB-TPA CMP.

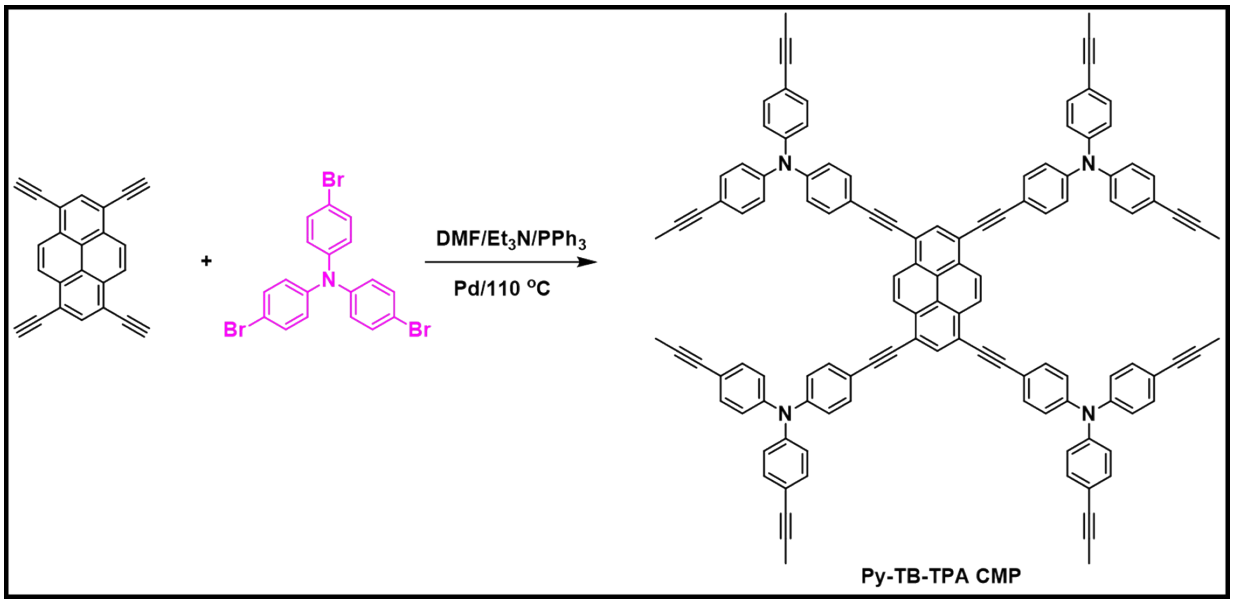

Scheme S12. Synthesis of Py-TB-TPA CMP.

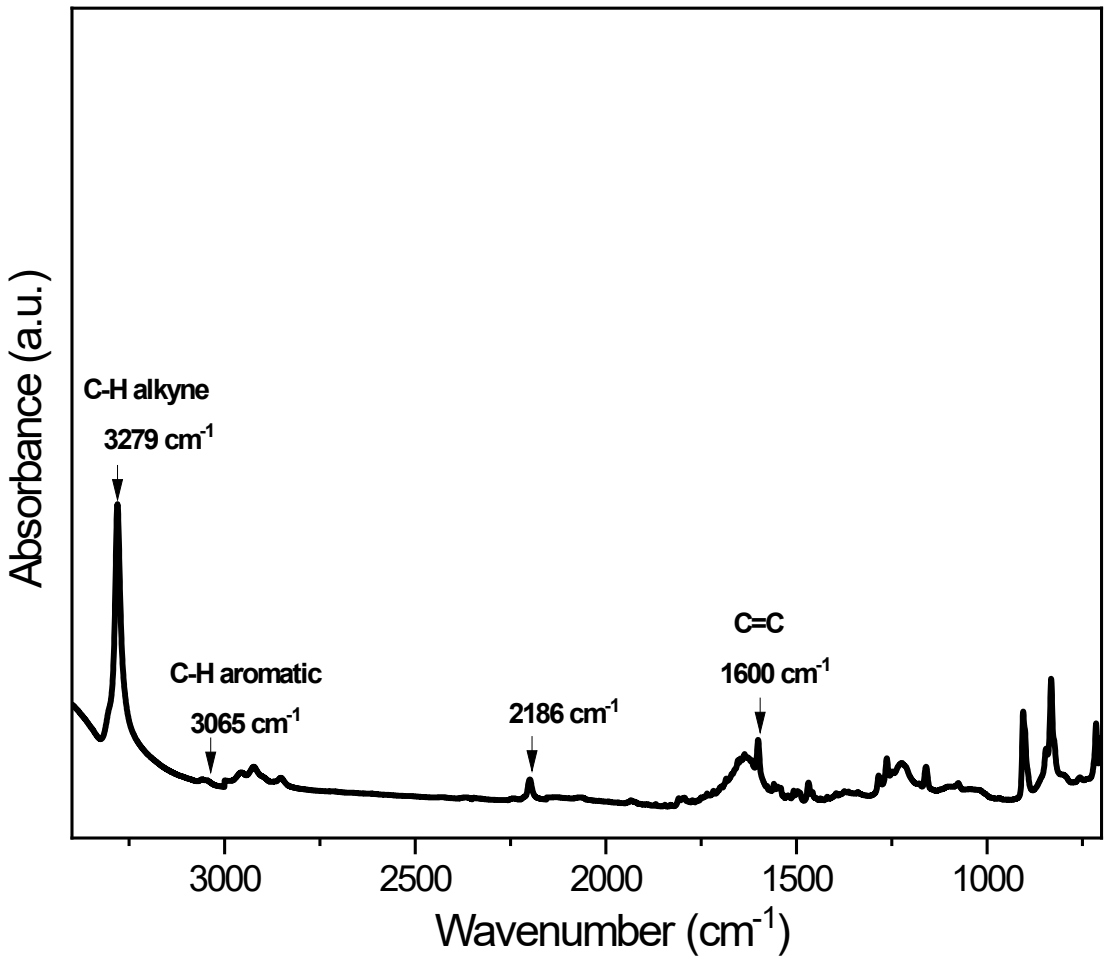

Figure S1. FT-IR spectrum of Py-T.

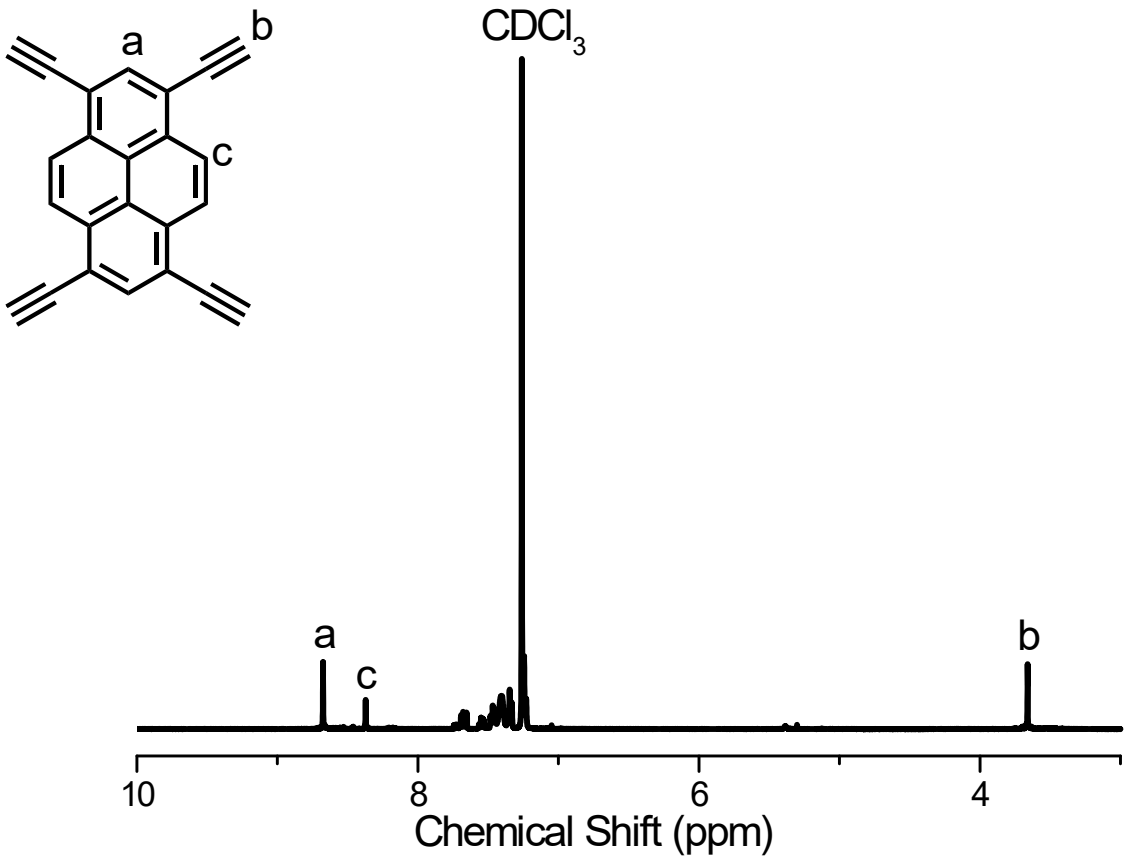

Figure S2. ^{1}H NMR spectrum of Py-T.

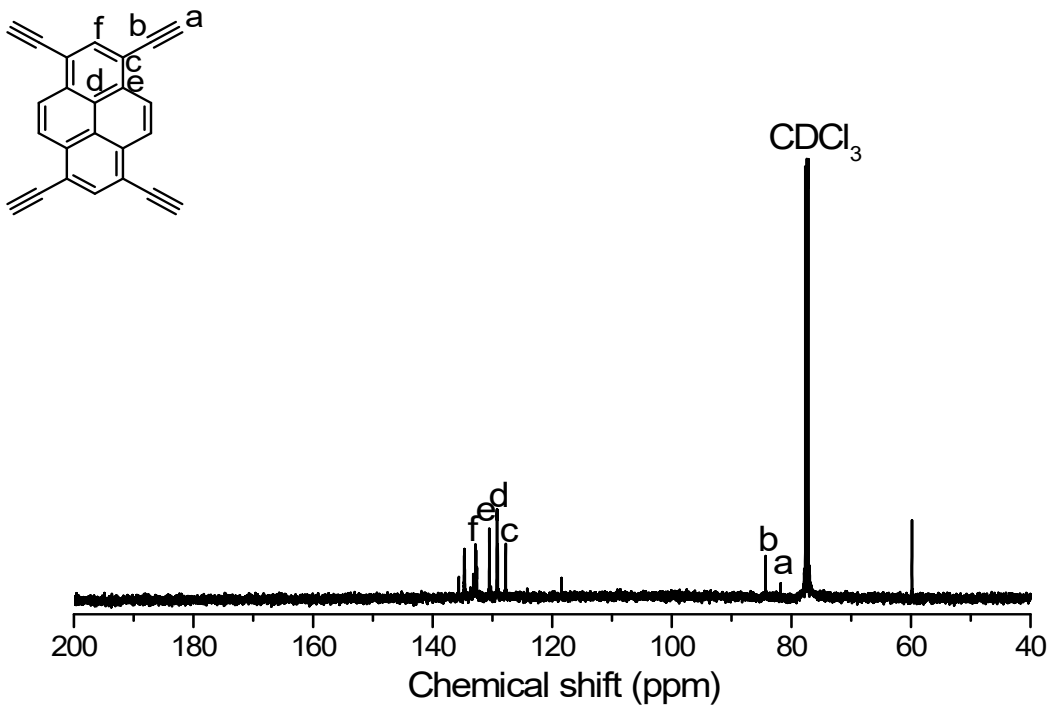

Figure S3. ^{13}C NMR spectrum of Py-T.

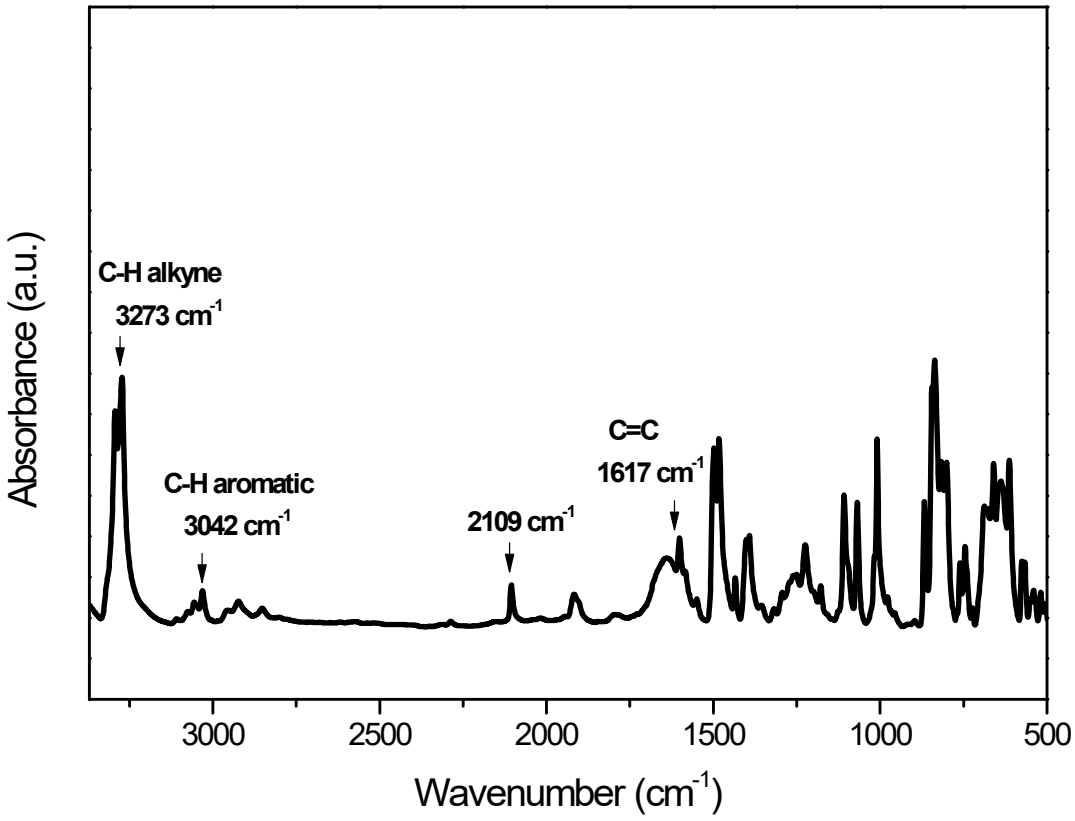

Figure S4. FT-IR spectrum of TPE-T.

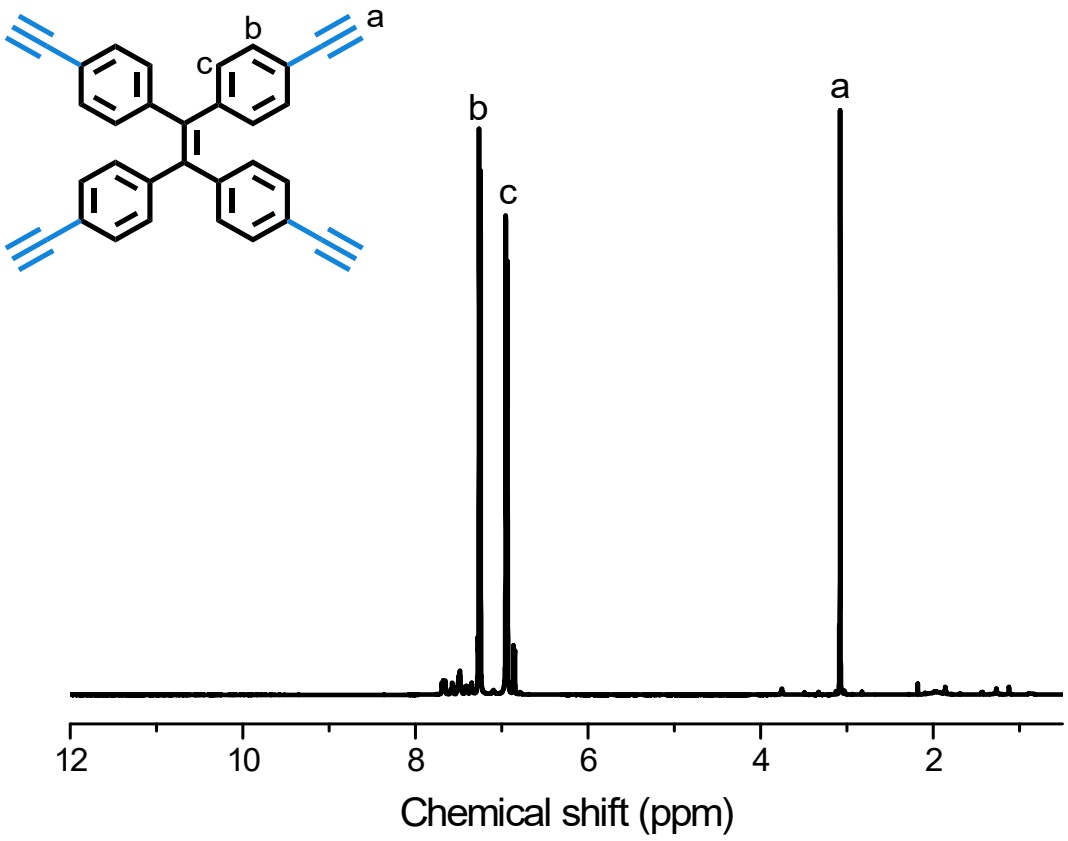

Figure S5. ^{1}H NMR spectrum of TPE-T.

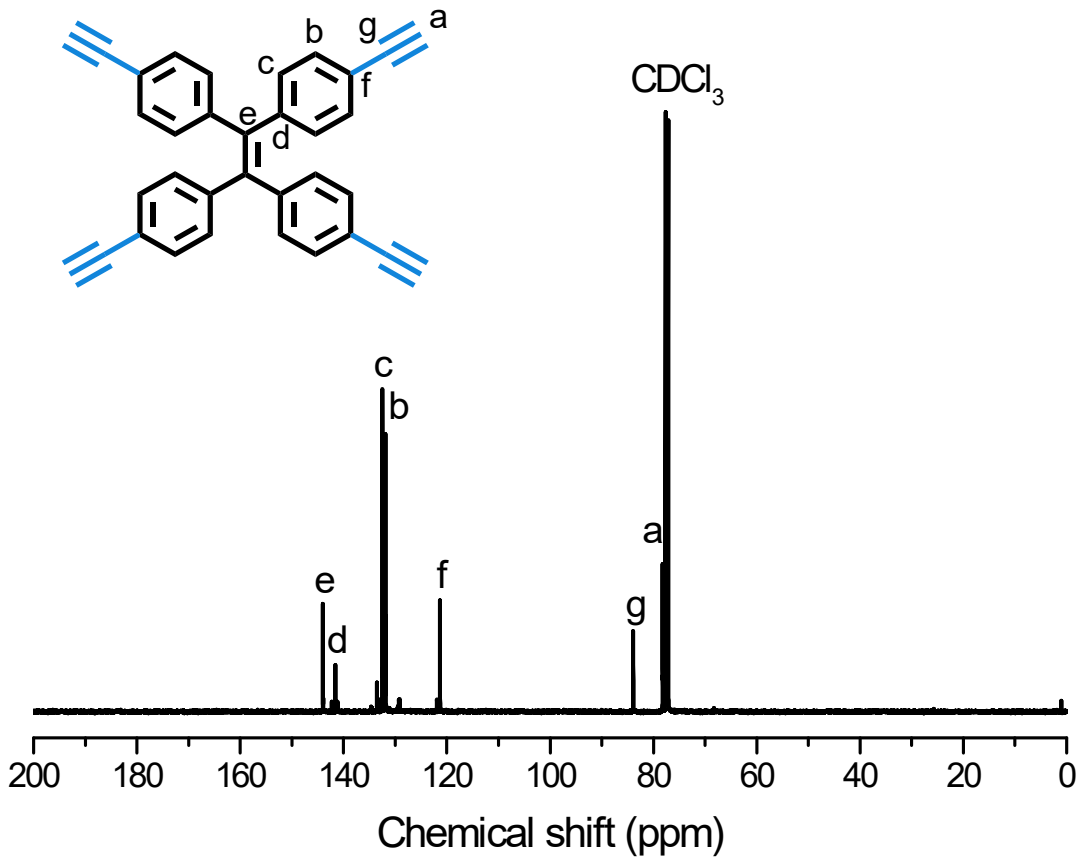

Figure S6. ^{13}C NMR spectrum of TPE-T.

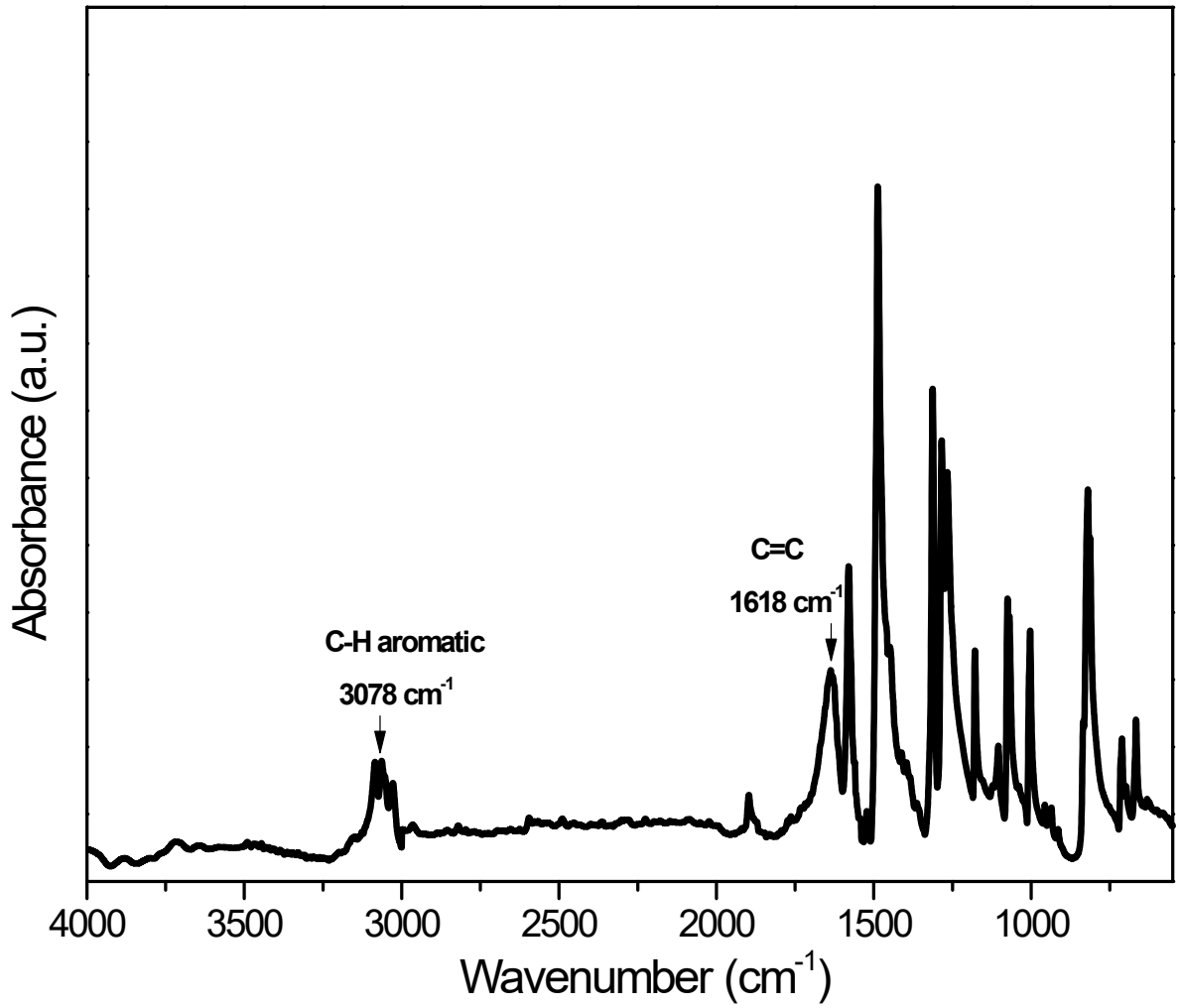

Figure S7. FT-IR spectrum of TPA-3Br.

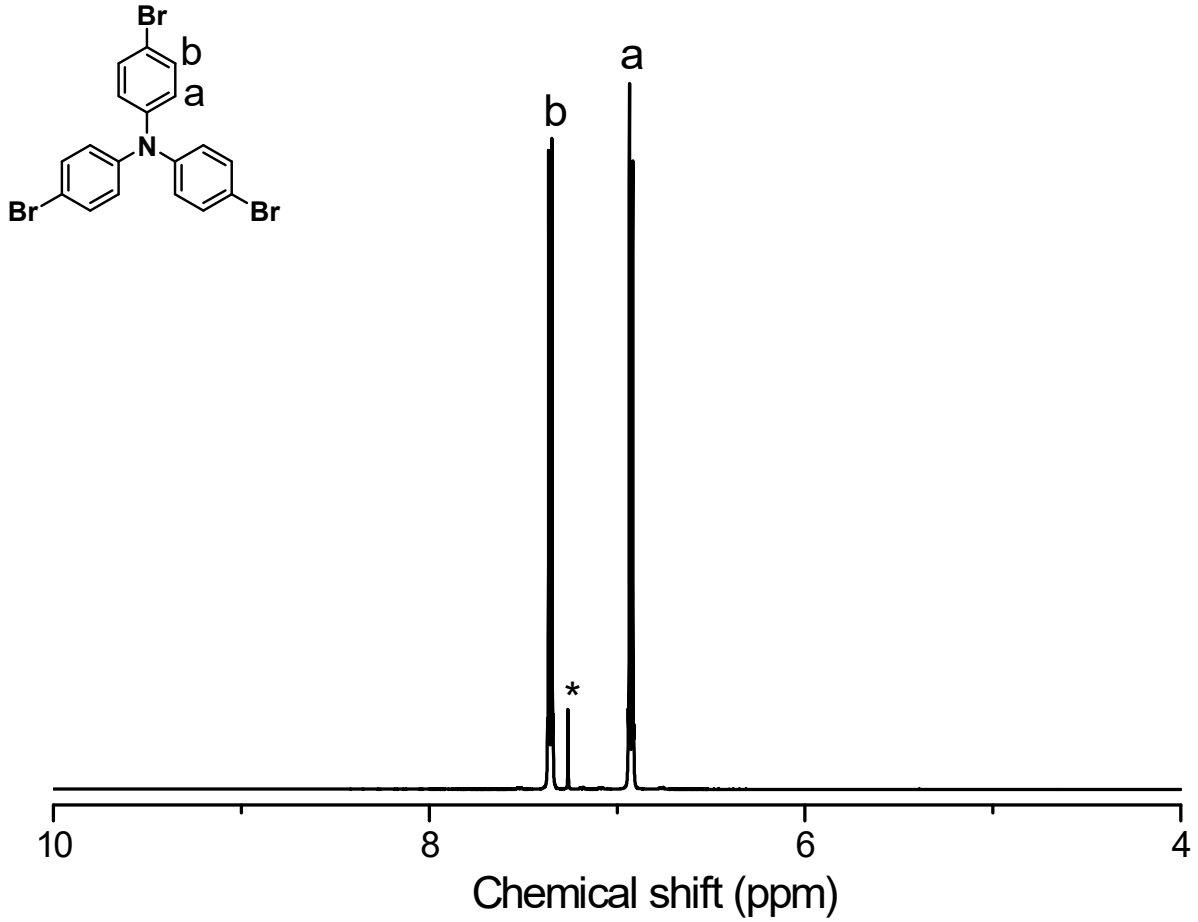

Figure S8. ^{1}H NMR spectrum of TPA-3Br. * is the peak for $CDCl_3$.

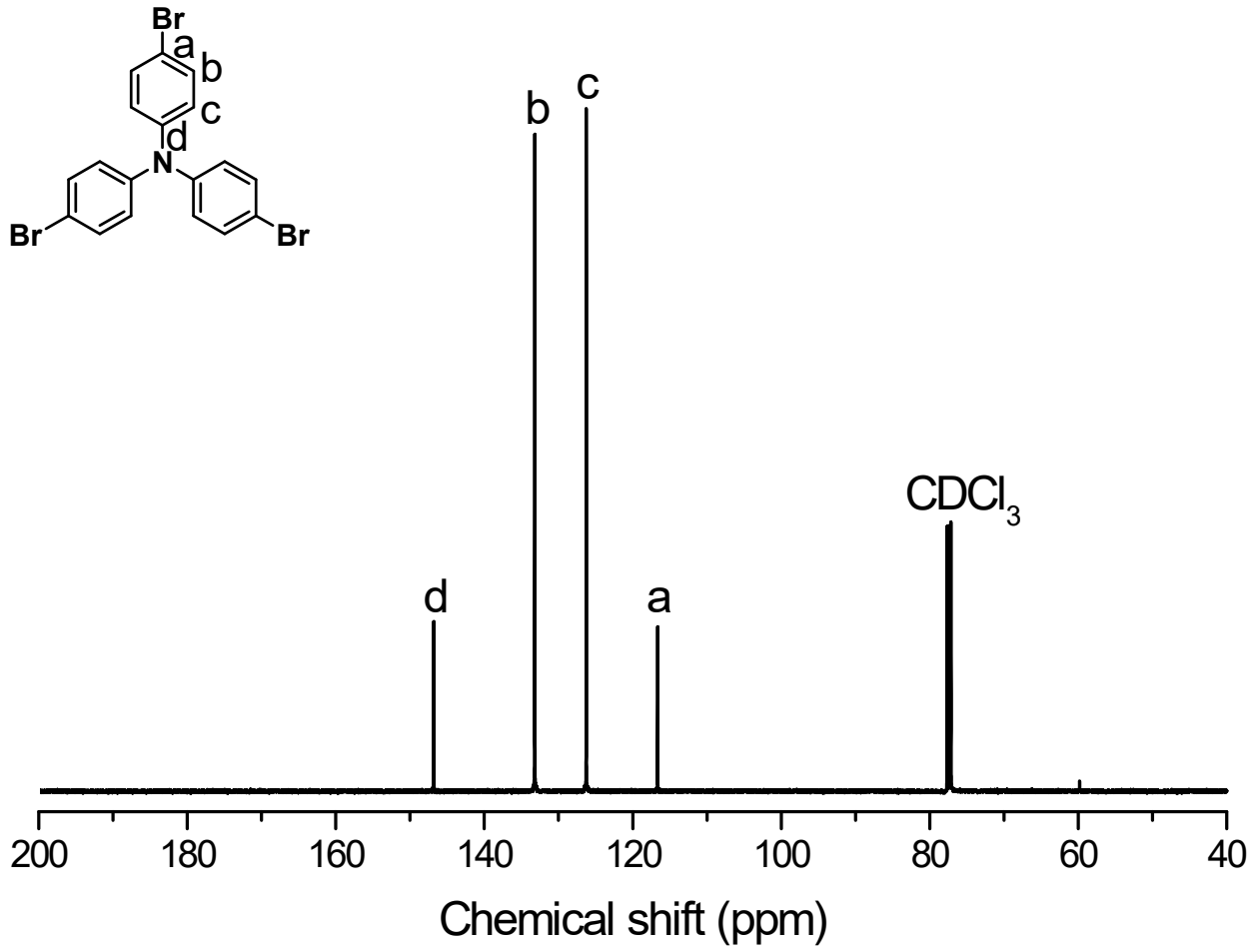

Figure S9. ^{13}C NMR spectrum of TPA-3Br.

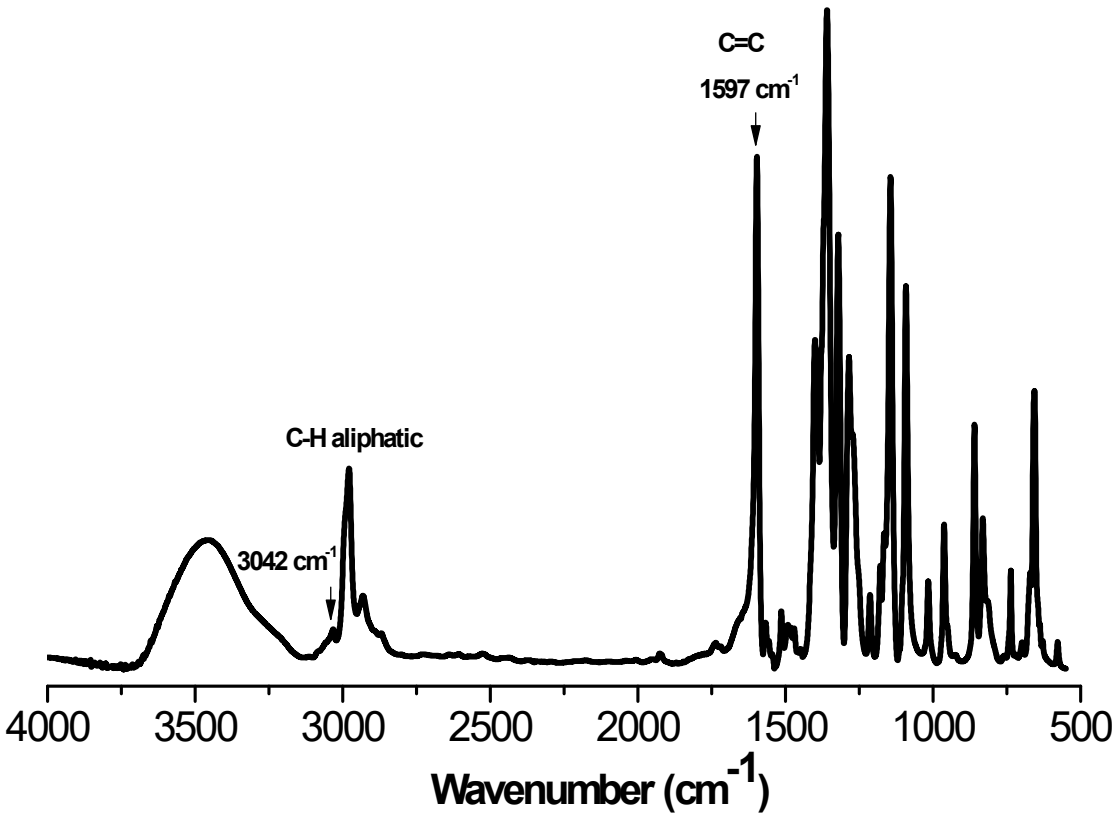

Figure S10. FT-IR spectrum of TPA-3B$(OCH_3)_2$.

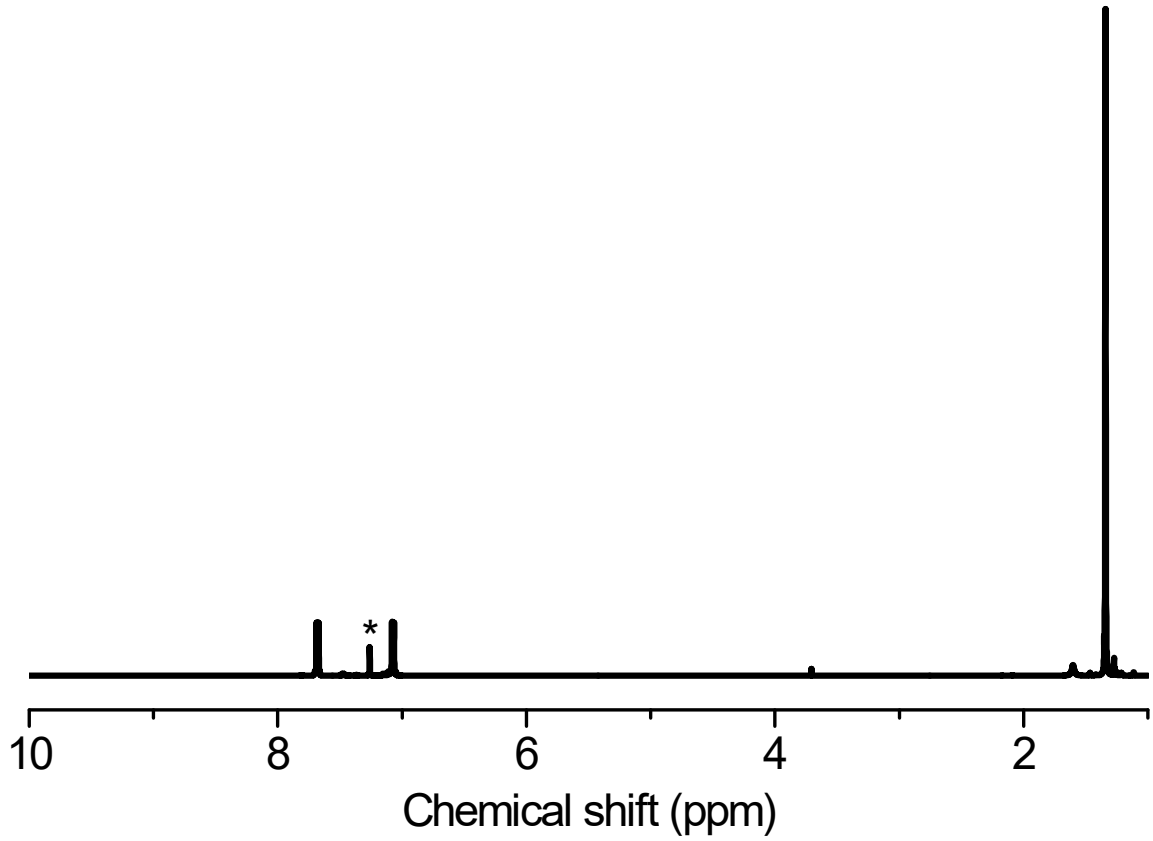

Figure S11. ^{1}H NMR spectrum of TPA-3B$(OCH_3)_2$. * is the peak for $CDCl_3$.

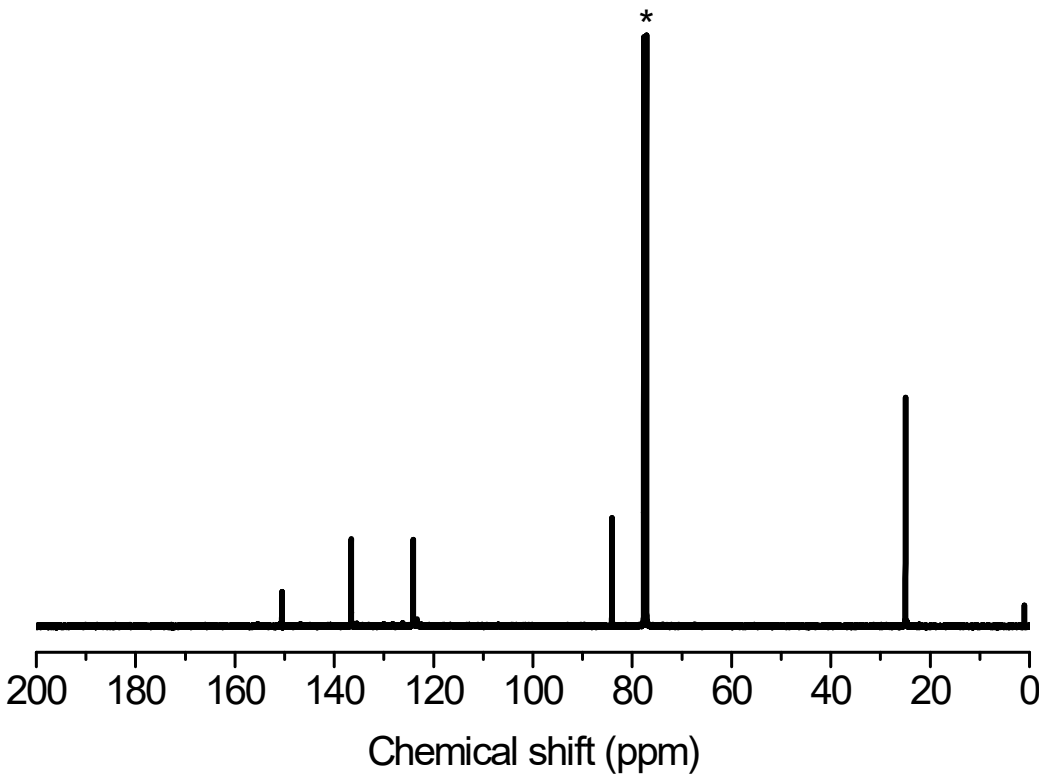

Figure S12. ^{13}C NMR spectrum of TPA-3B$(OCH_3)_2$. * is the peak for $CDCl_3$.

.

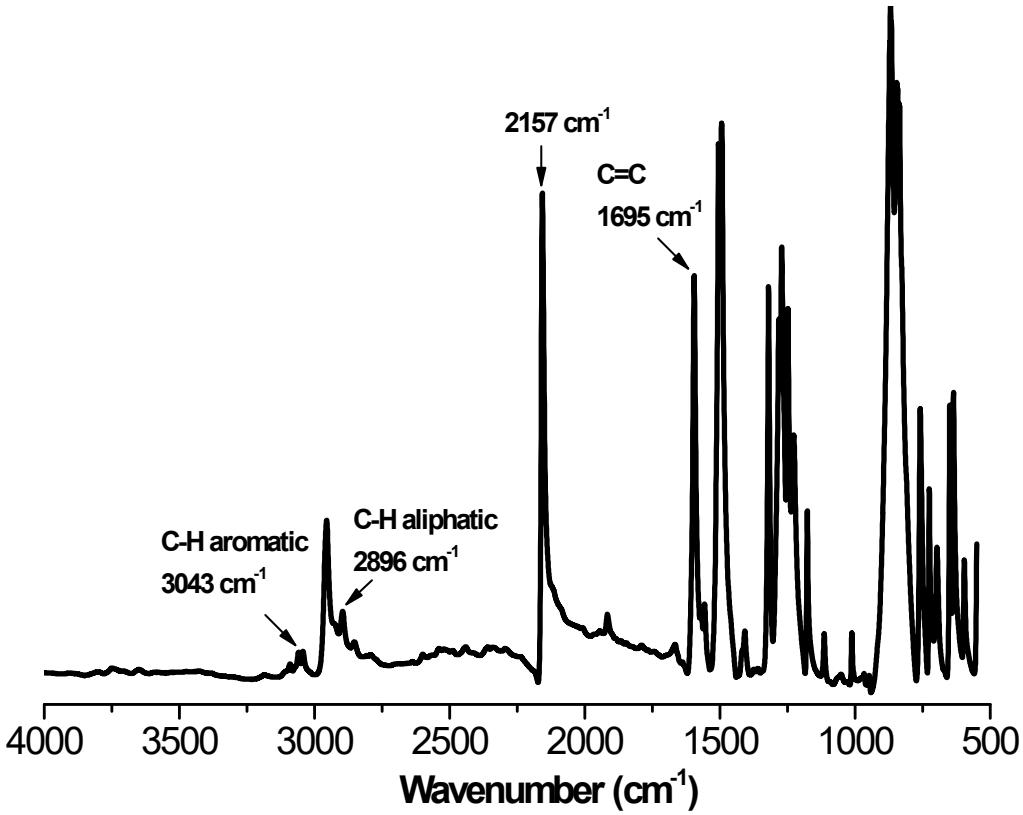

Figure S13. FT-IR spectrum of TPA-TMS.

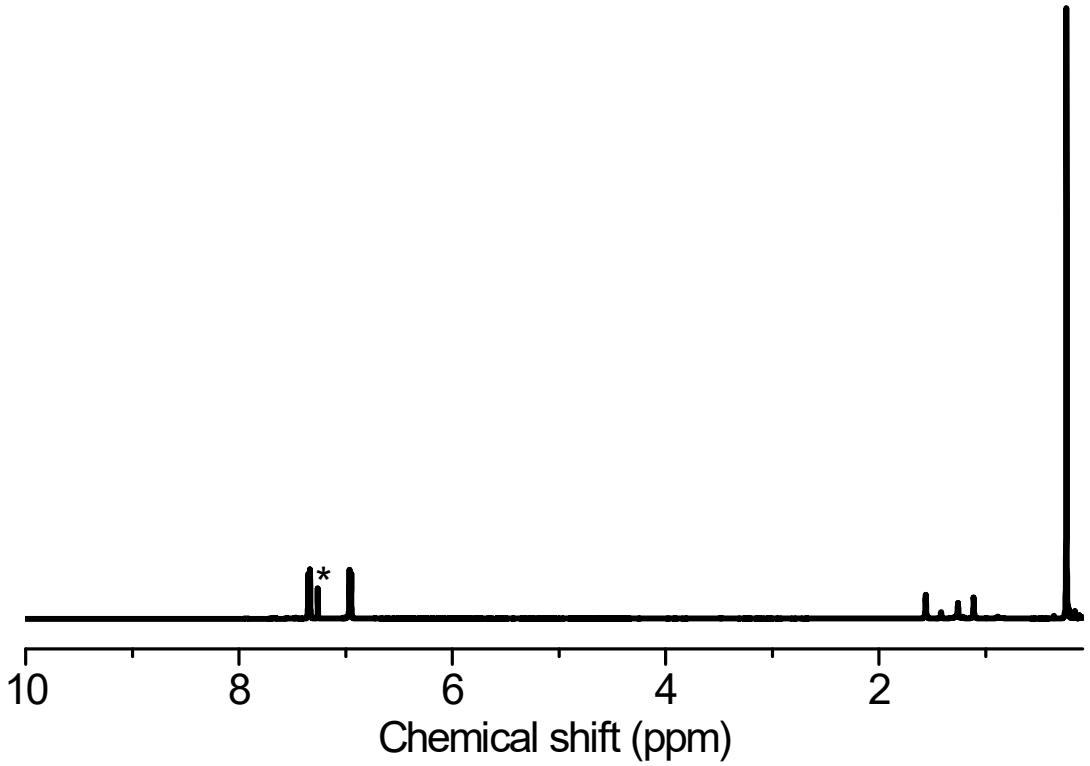

Figure S14. ^{1}H NMR spectrum of TPA-TMS. * is the peak for $CDCl_3$.

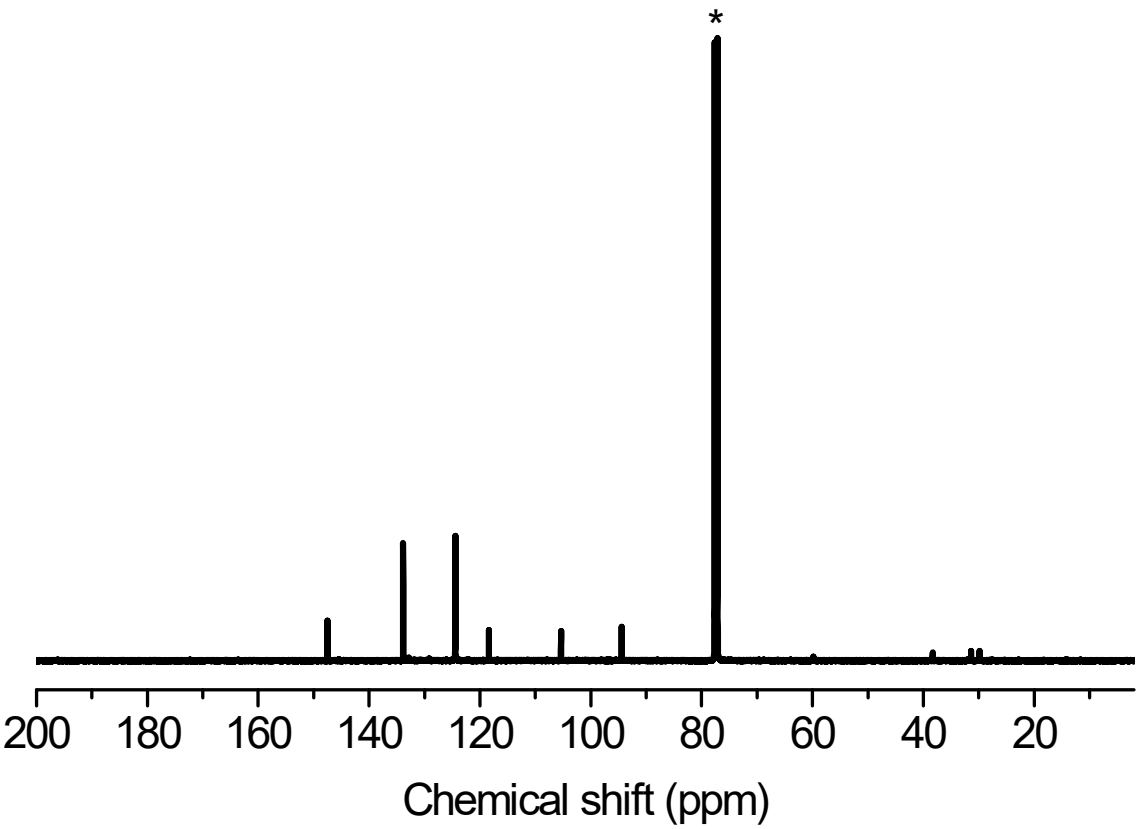

Figure S15. ^{13}C NMR spectrum of TPA-TMS. * is the peak for $CDCl_3$.

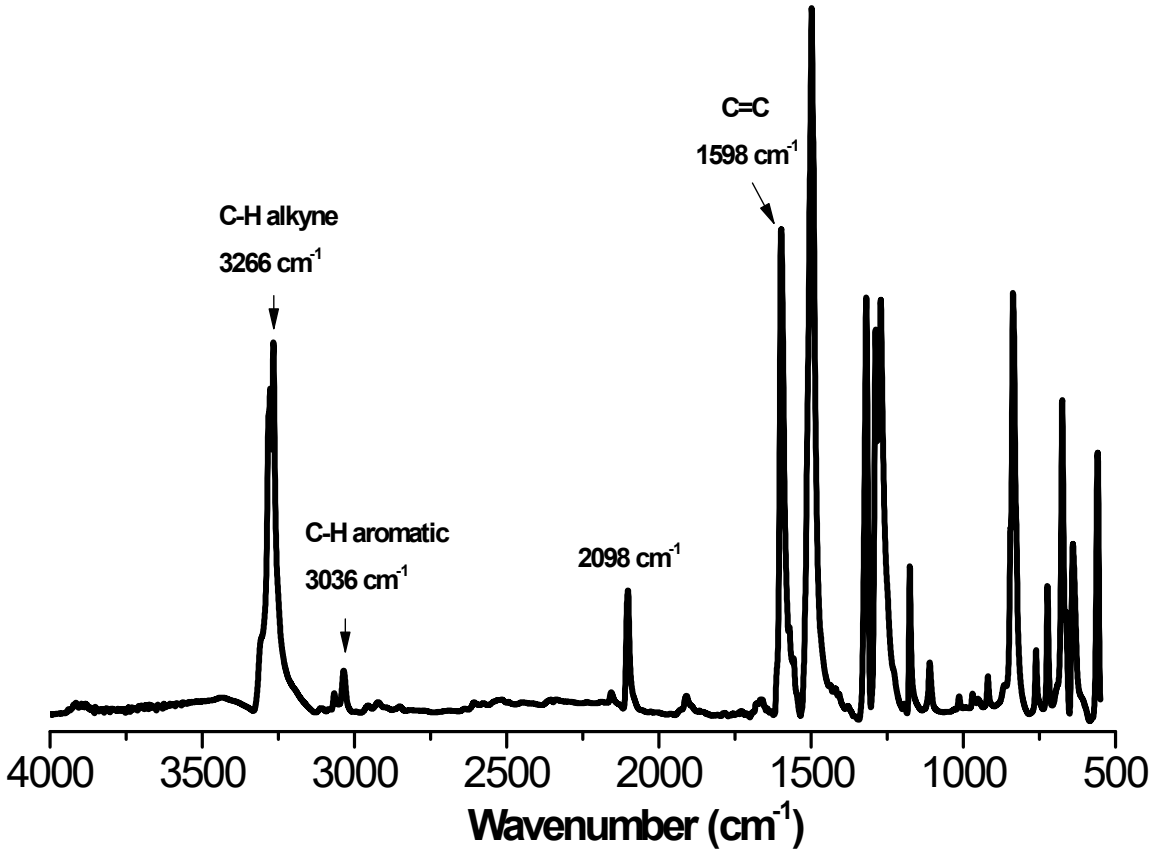

Figure S16. FT-IR spectrum of TPA-T.

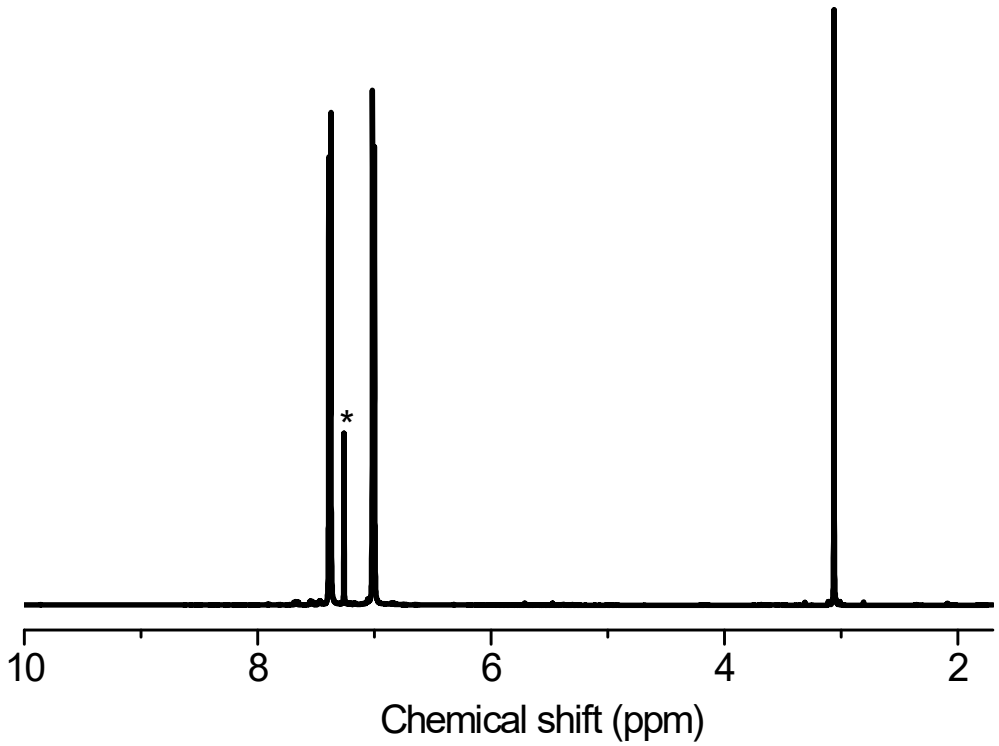

Figure S17. ^{1}H NMR spectrum of TPA-T. * is the peak for $CDCl_3$.

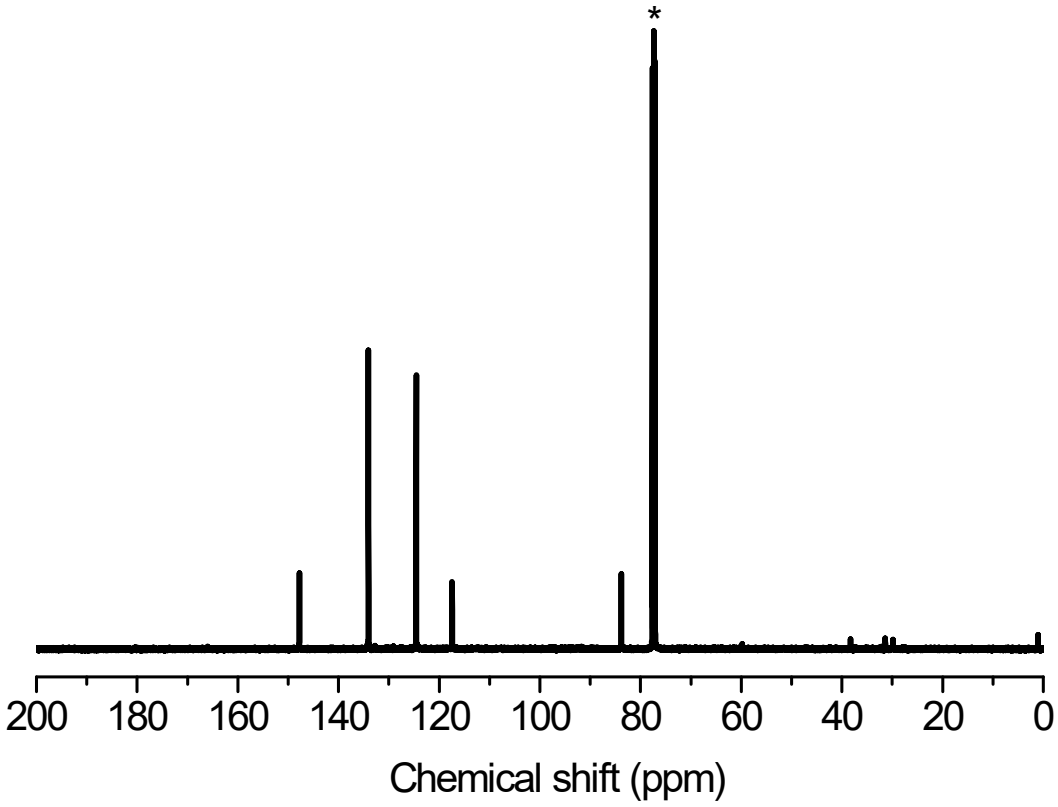

Figure S18. ^{13}C NMR spectrum of TPA-T. * is the peak for $CDCl_3$.

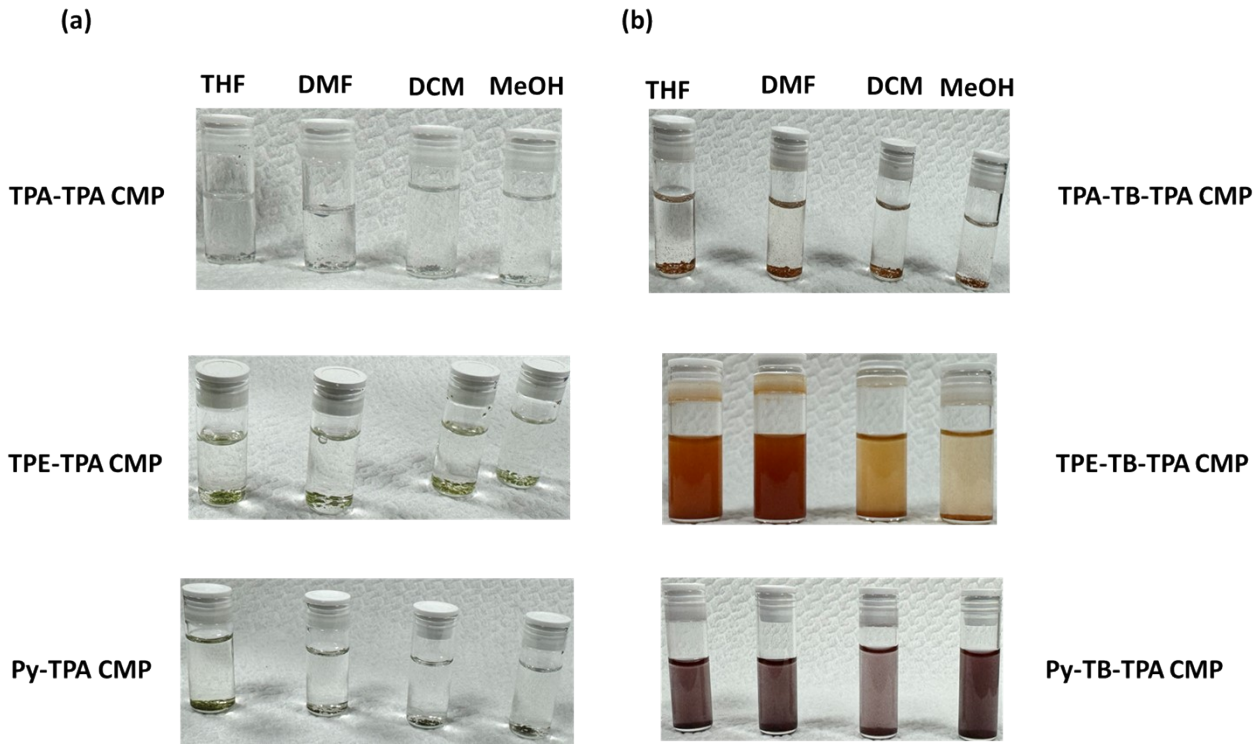

Figure S19. Solubility test of (a) TPA-TPA CMP, TPE-TPA CMP, and Py-TPA CMP and (b) TPA-TB-TPA CMP, TPE-TB-TPA CMP, and Py-TB-TPA CMP in THF, DMF, DCM and MeOH; respectively.

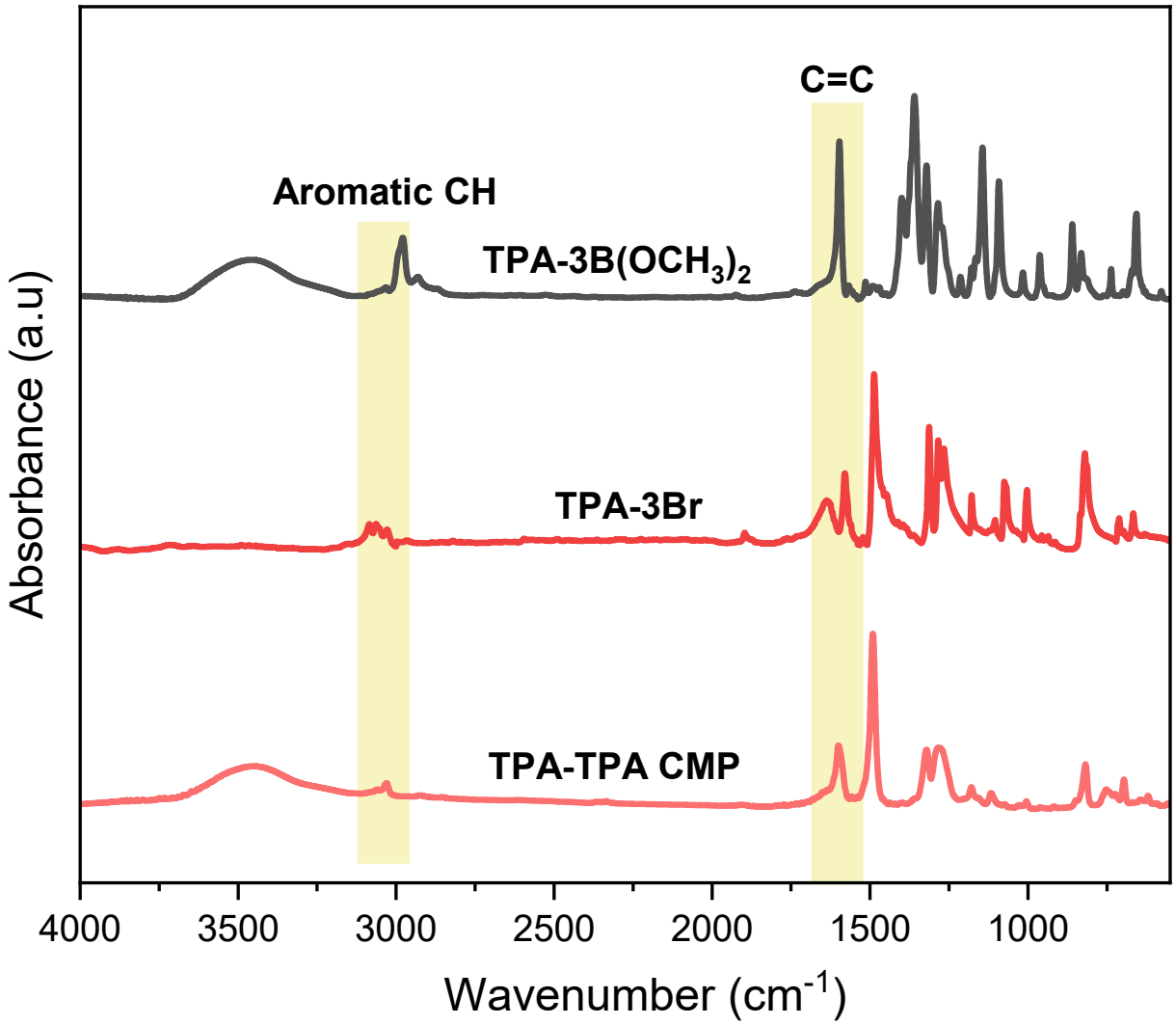

Figure S20. FTIR profiles of TPA-3B$(OCH_3)_2$, TPA-3Br and TPA-TPA CMP, were recorded at room temperature.

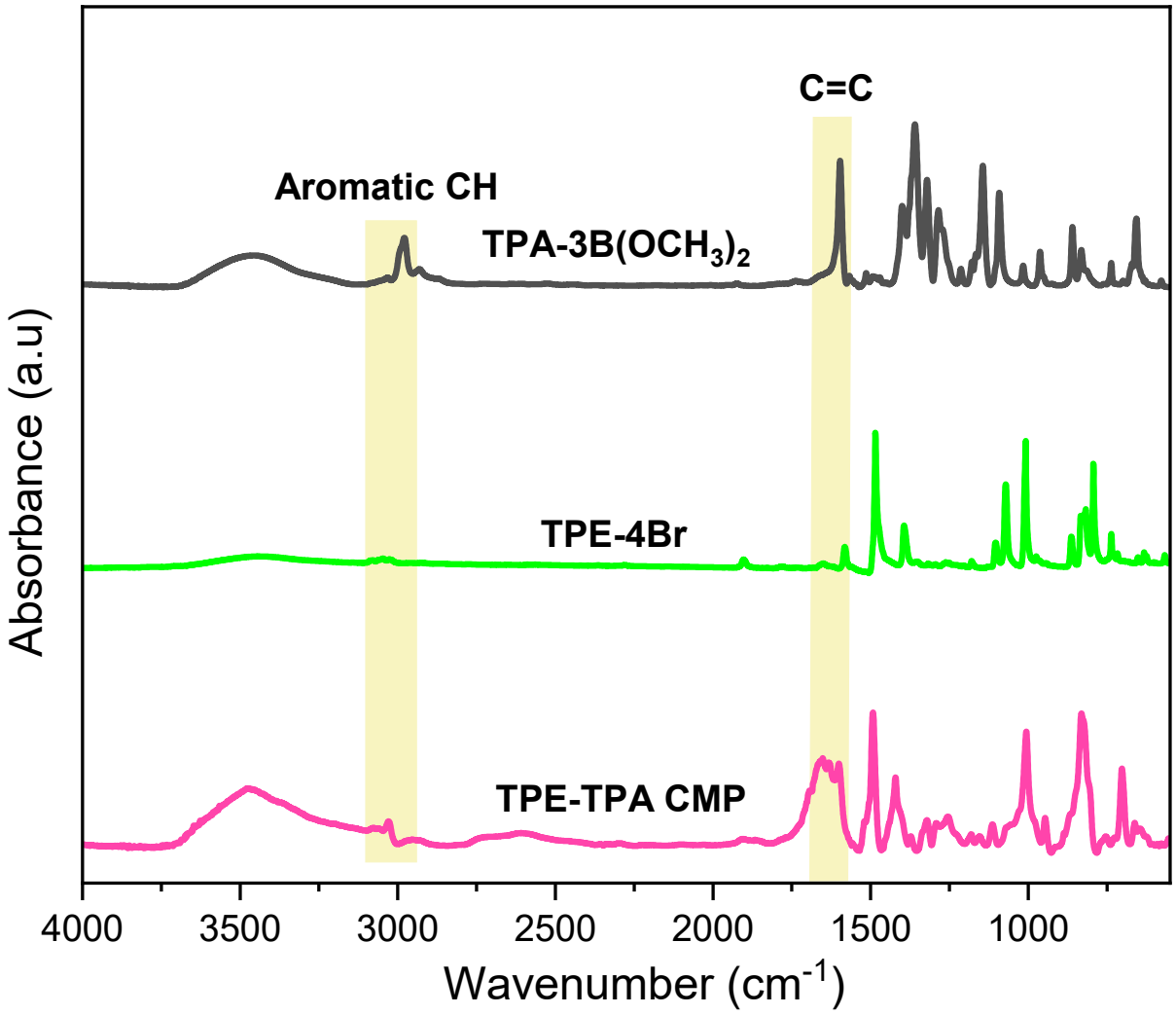

Figure S21. FTIR profiles of TPA-3B$(OCH_3)_2$, TPE-4Br, and TPE-TPA CMP, were recorded at room temperature.

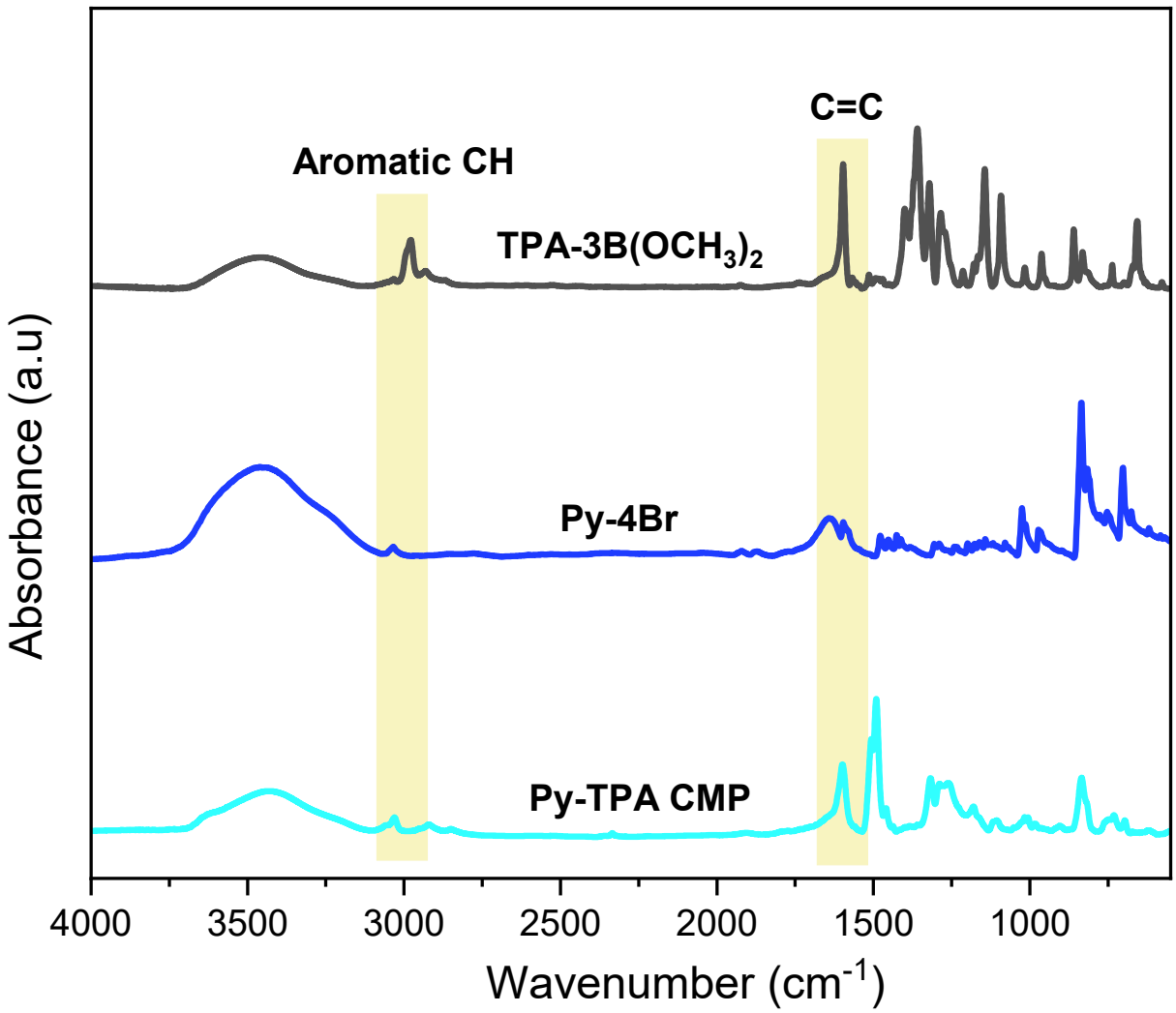

Figure S22. FTIR profiles of TPA-3B$(OCH_3)_2$, Py-4Br and Py-TPA CMP, were recorded at room temperature.

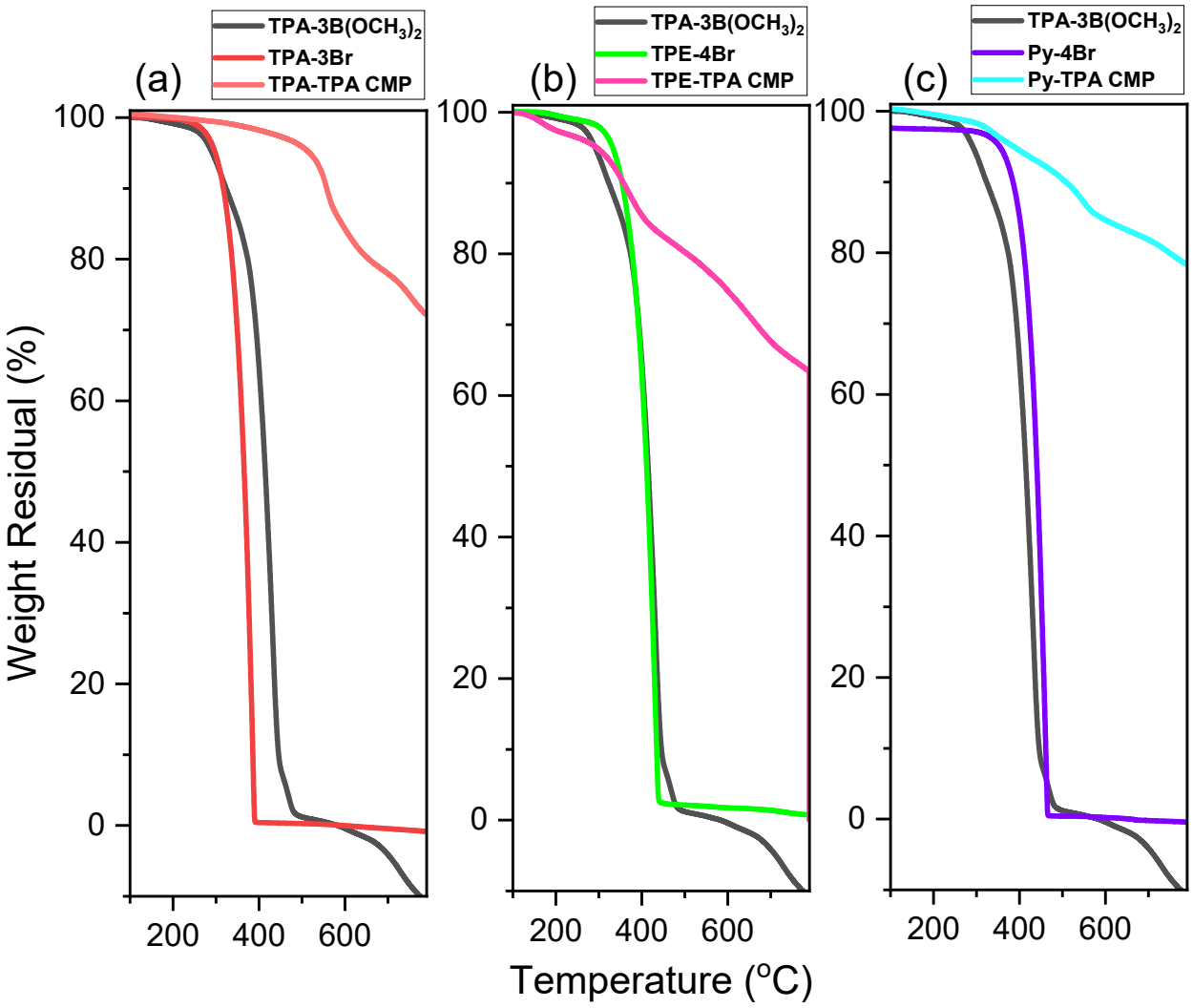

Figure S23. TGA profiles of (a) TPA-3B$(OCH_3)_2$, TPA-3Br and TPA-TPA CMP, (b) (a) TPA-3B$(OCH_3)_2$, TPE-4Br and TPE-TPA CMP and (c) TPA-3B$(OCH_3)_2$, Py-4Br and Py-TPA CMP.

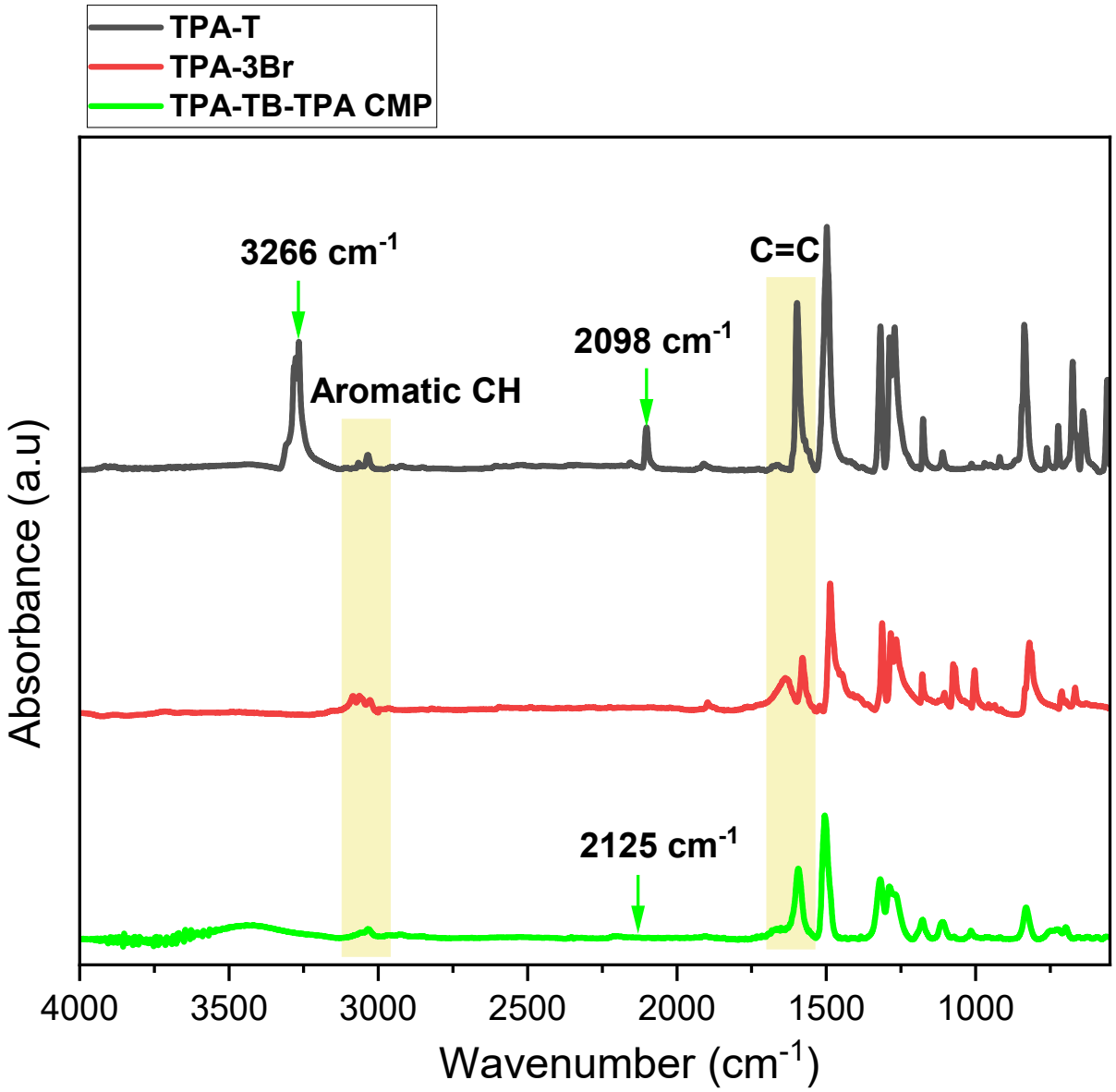

Figure S24. FTIR profiles of TPA-T, TPA-3Br, and TPA-TB-TPA CMP, were recorded at room temperature.

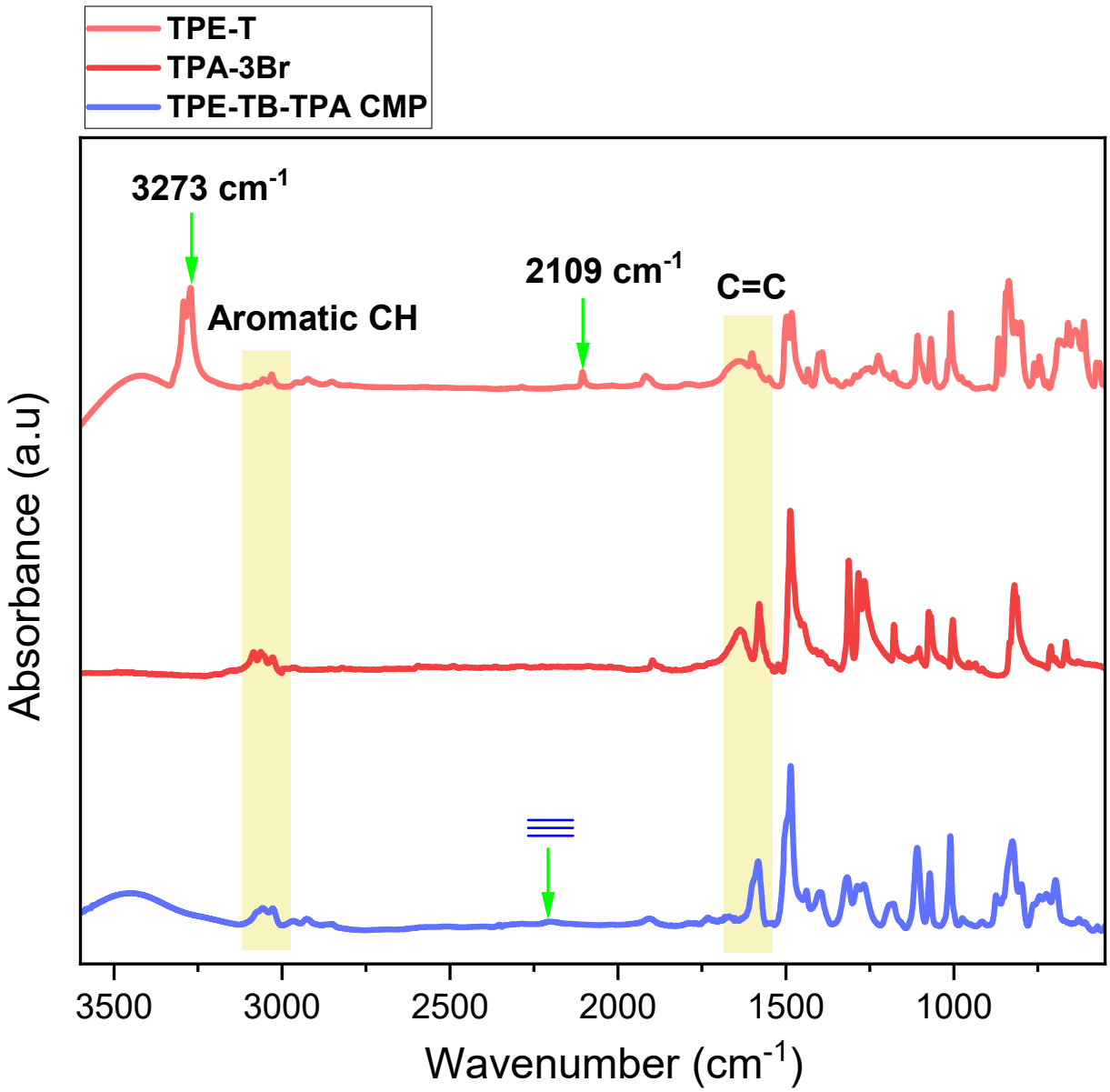

Figure S25. FTIR profiles of TPE-T, TPA-3Br and TPE-TB-TPA CMP, were recorded at room temperature.

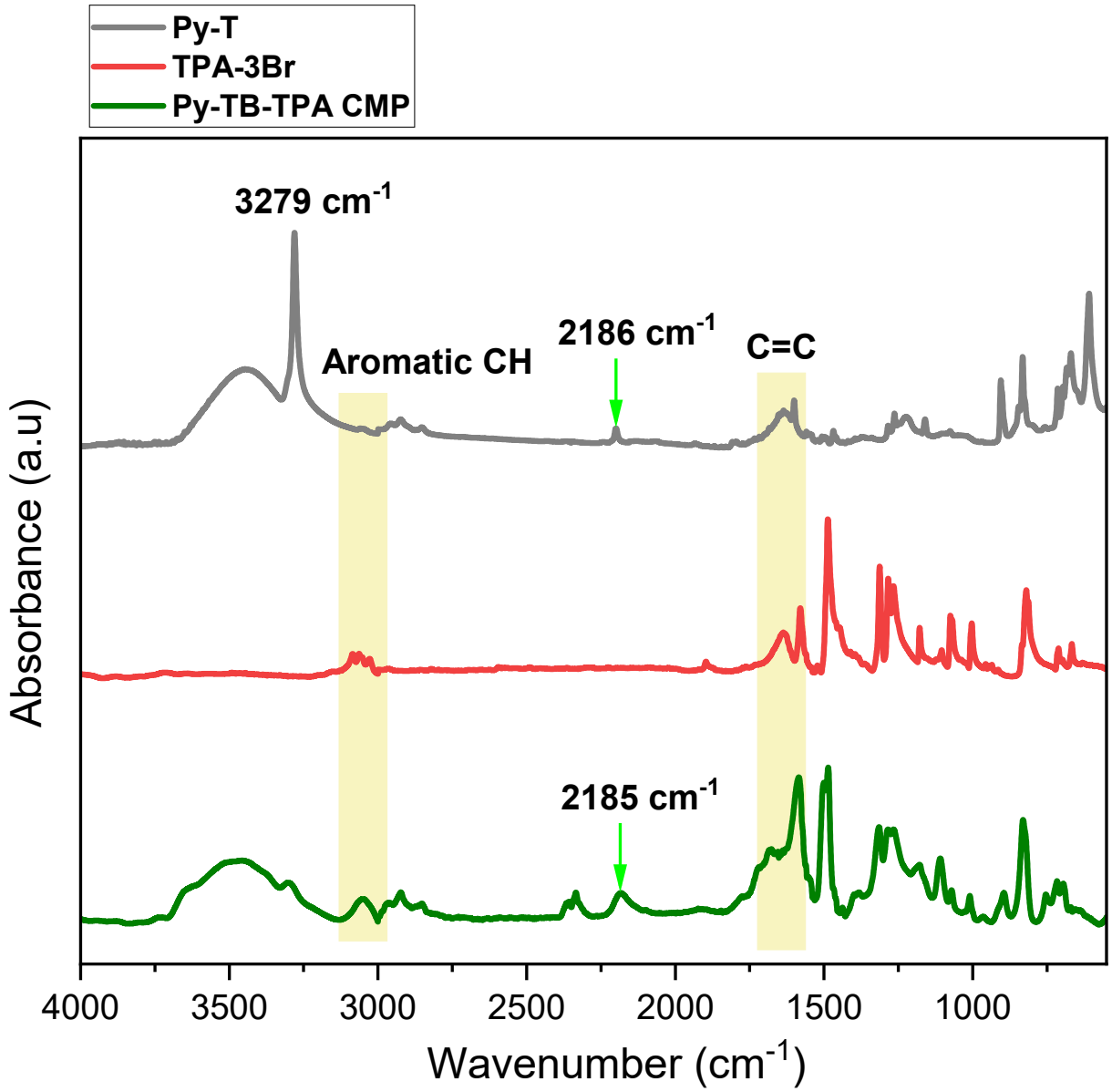

Figure S26. FTIR profiles of Py-T, TPA-3Br and Py-TB-TPA CMP, were recorded at room temperature.

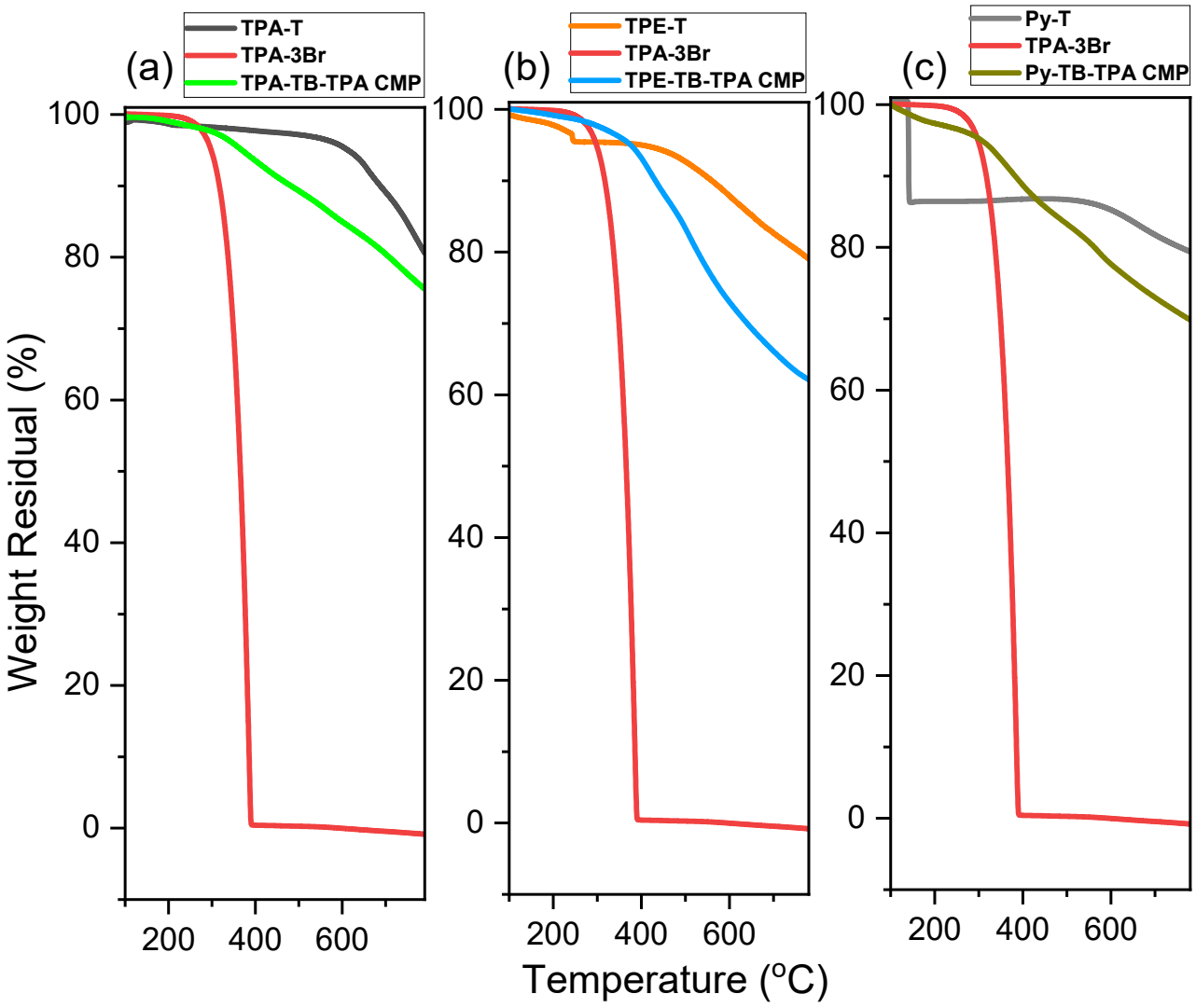

Figure S27. TGA profiles of (a) TPA-T, TPA-3Br, and TPA-TB-TPA CMP, (b) (a) TPE-T, TPA-3Br, and TPE-TB-TPA CMP, and (c) Py-T, TPA-3Br and Py-TB-TPA CMP.

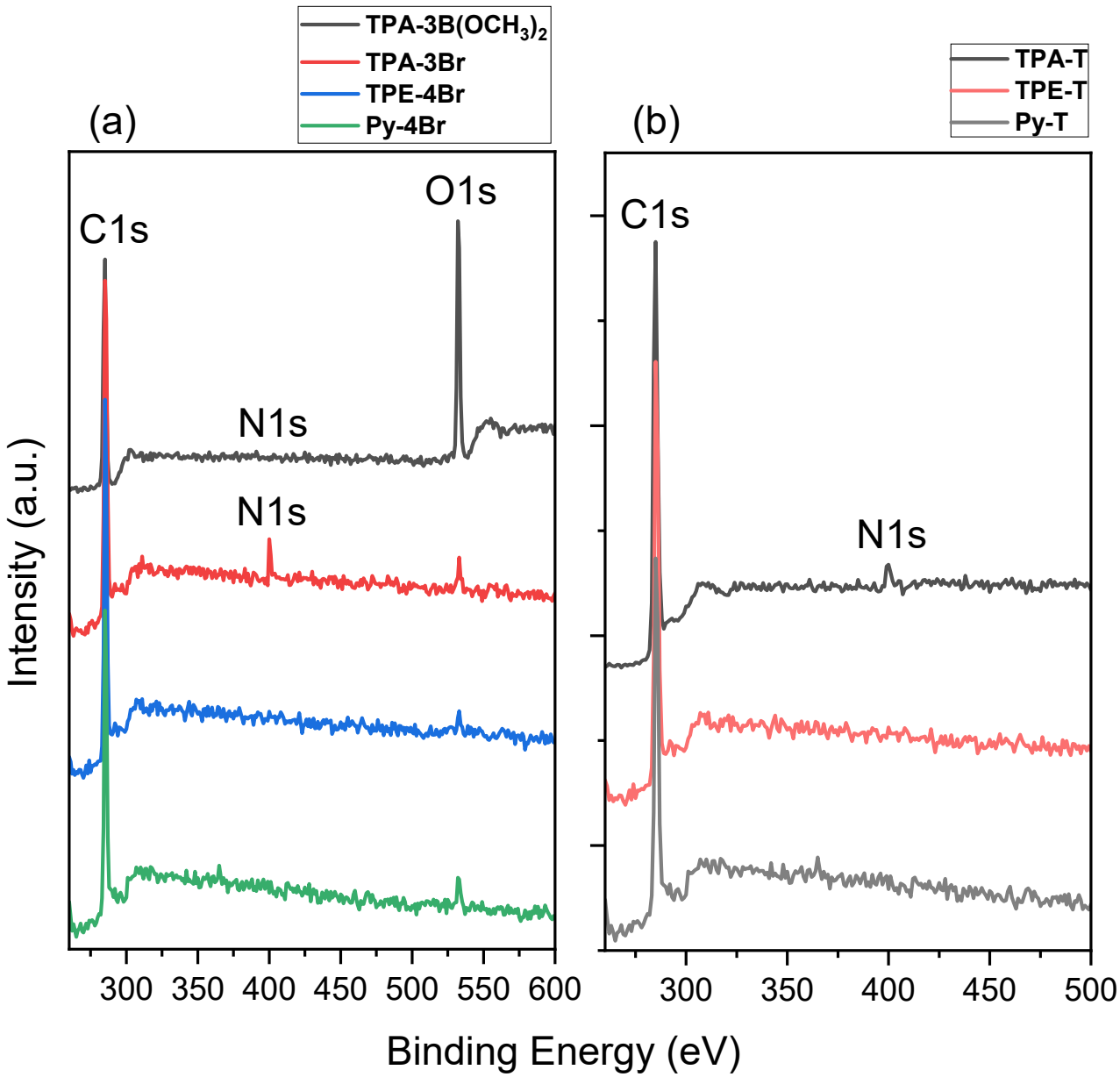

Figure S28. XPS spectra of (a) TPA-3B$(OCH_3)_2$, TPA-3Br, TPE-4Br and Py-4Br and (b) TPA-T, TPE-T, and Py-T.

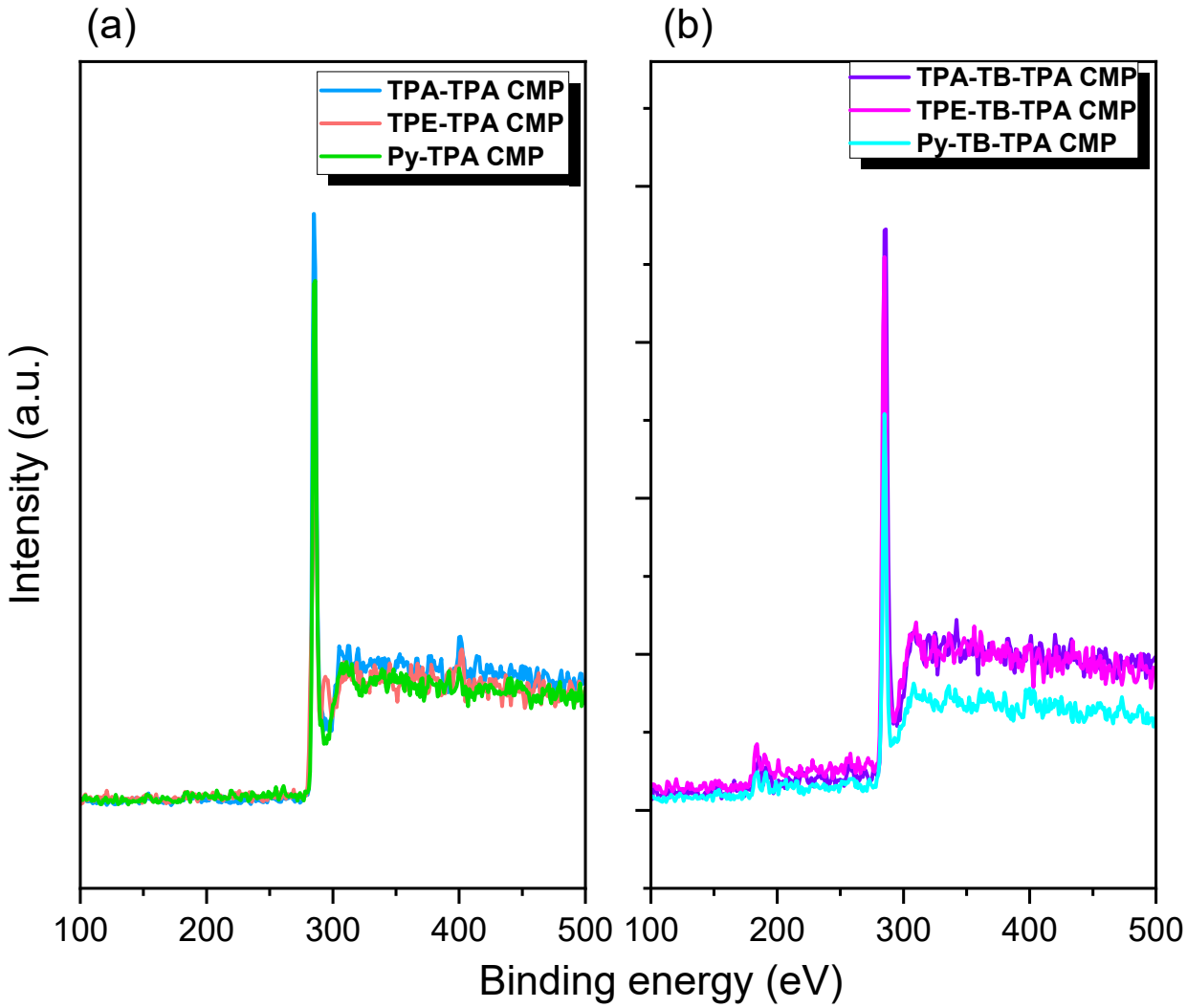

Figure S29. XPS spectra of (a) TPA-TPA CMP, TPE-TPA CMP and Py-TPA CMP and (b) TPA-TB-TPA CMP, TPE-TB-TPA CMP, and Py-TB-TPA CMP.

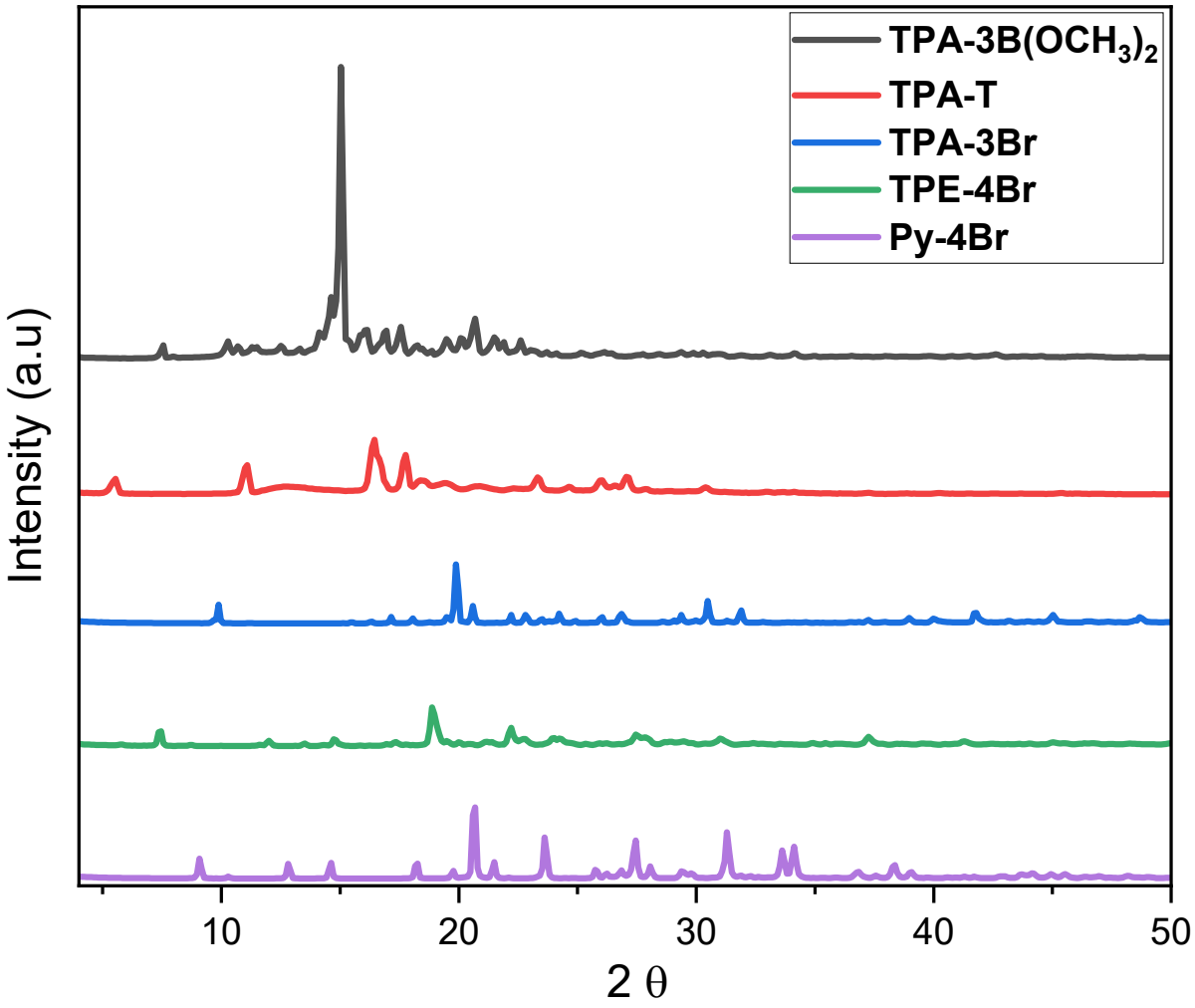

Figure S30. XRD profiles of TPA-3B$(OCH_3)_2$, TPA-T, TPA-3Br, TPE-4Br and Py-4Br, recorded at room temperature.

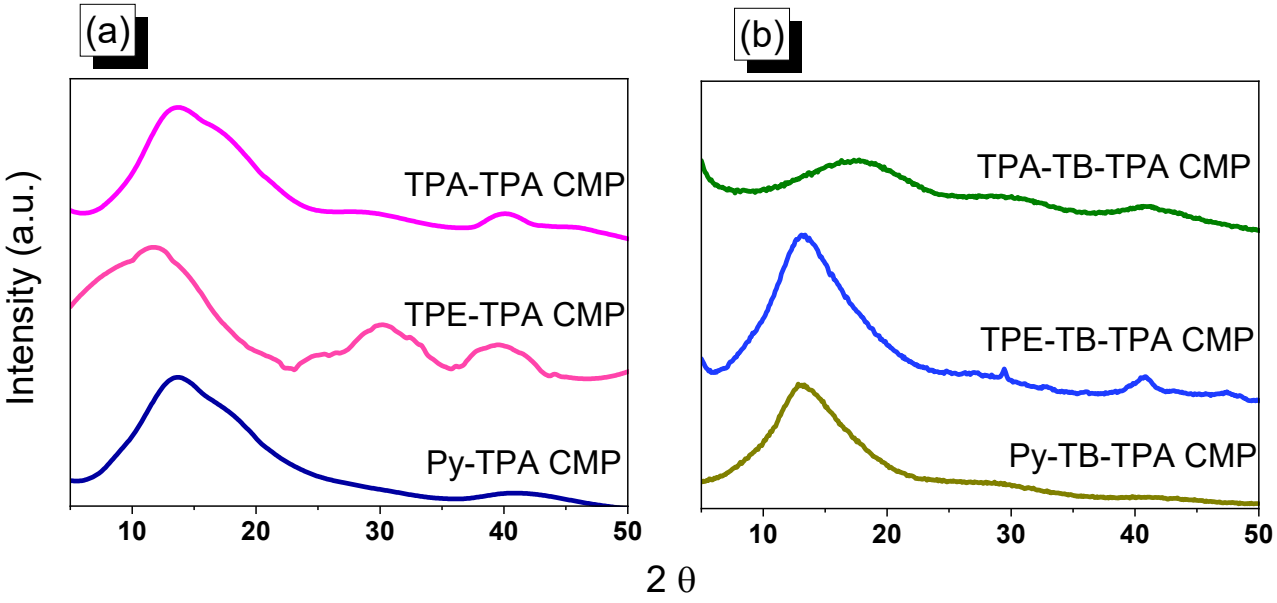

Figure S31. XRD spectra of (a) TPA-TPA CMP, TPE-TPA CMP, and Py-TPA CMP and (b) TPA-TB-TPA CMP, TPE-TB-TPA CMP, and Py-TB-TPA CMP.

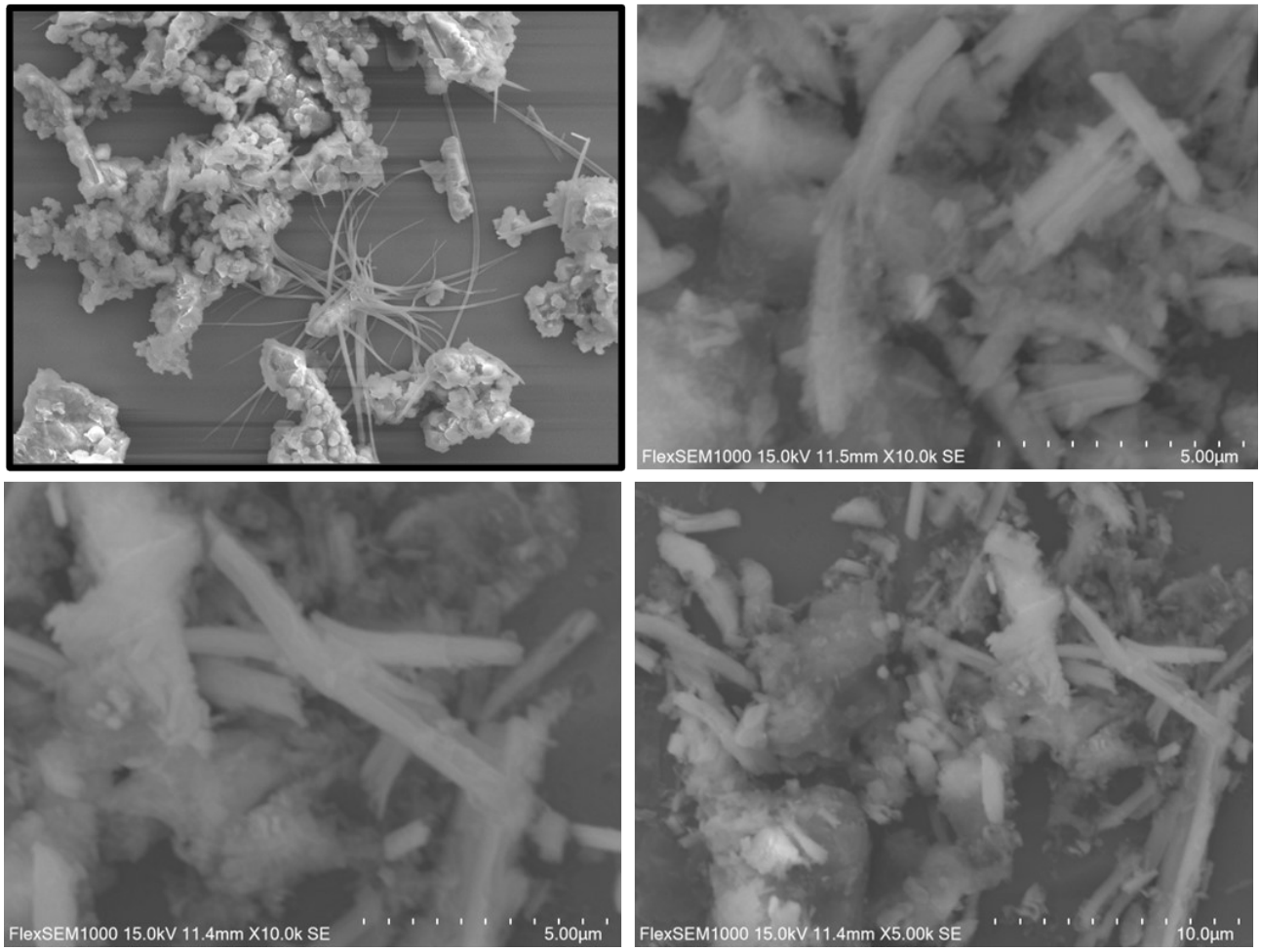

Figure S32. SEM images of Py-TPA CMP.

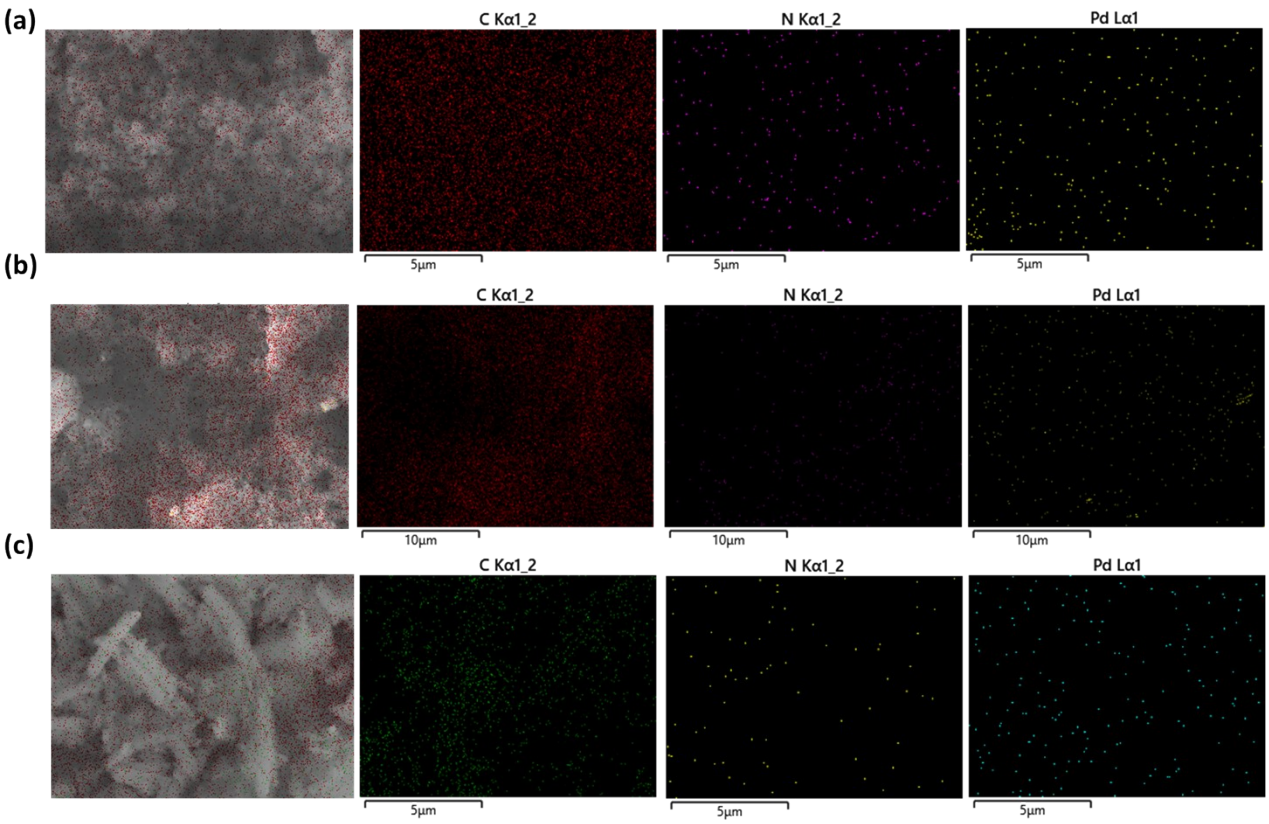

Figure S33. SEM-EDS mapping of (a) TPA-TPA CMP, (b) TPE-TPA CMP, and (c) Py-TPA CMP.

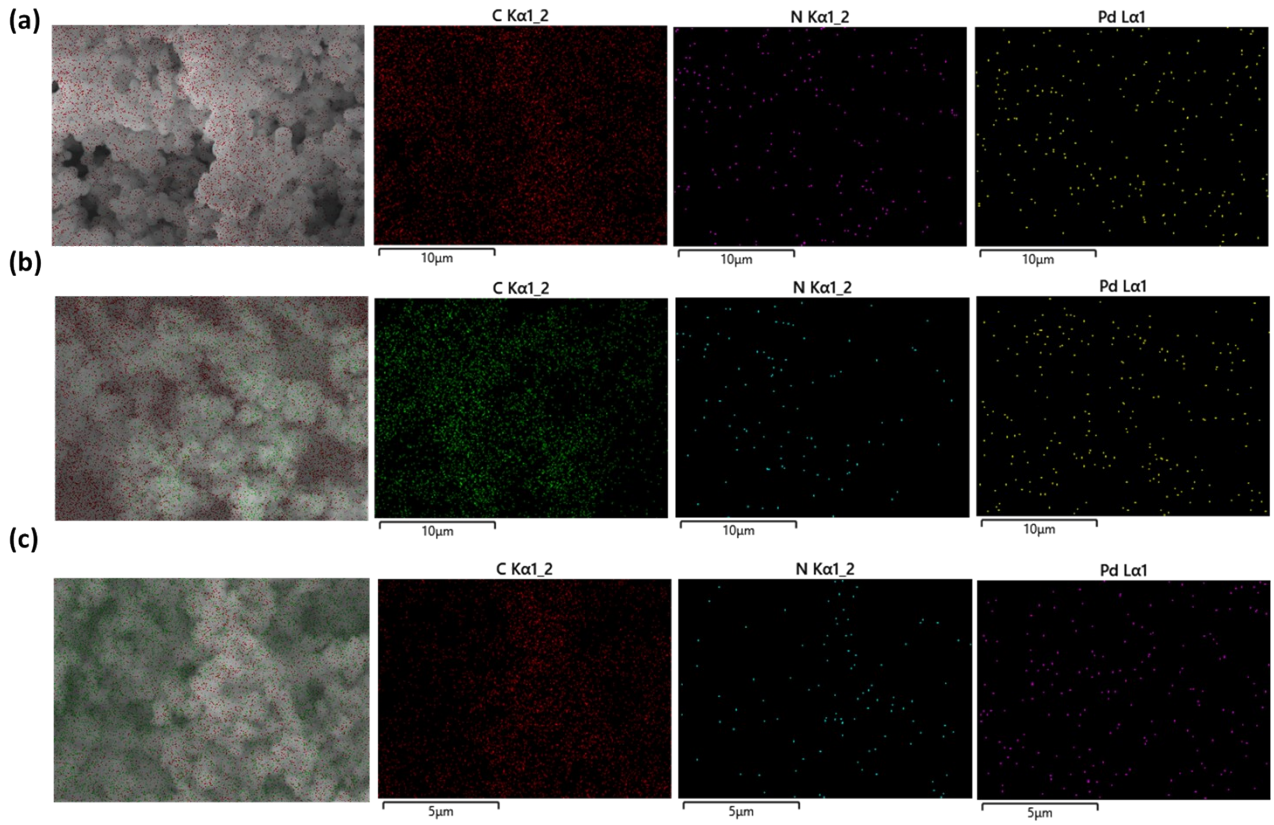

Figure S34. SEM-EDS mapping of (a) TPA-TB-TPA CMP, (b) TPE-TB-TPA CMP, and (c) Py-TB-TPA CMP.

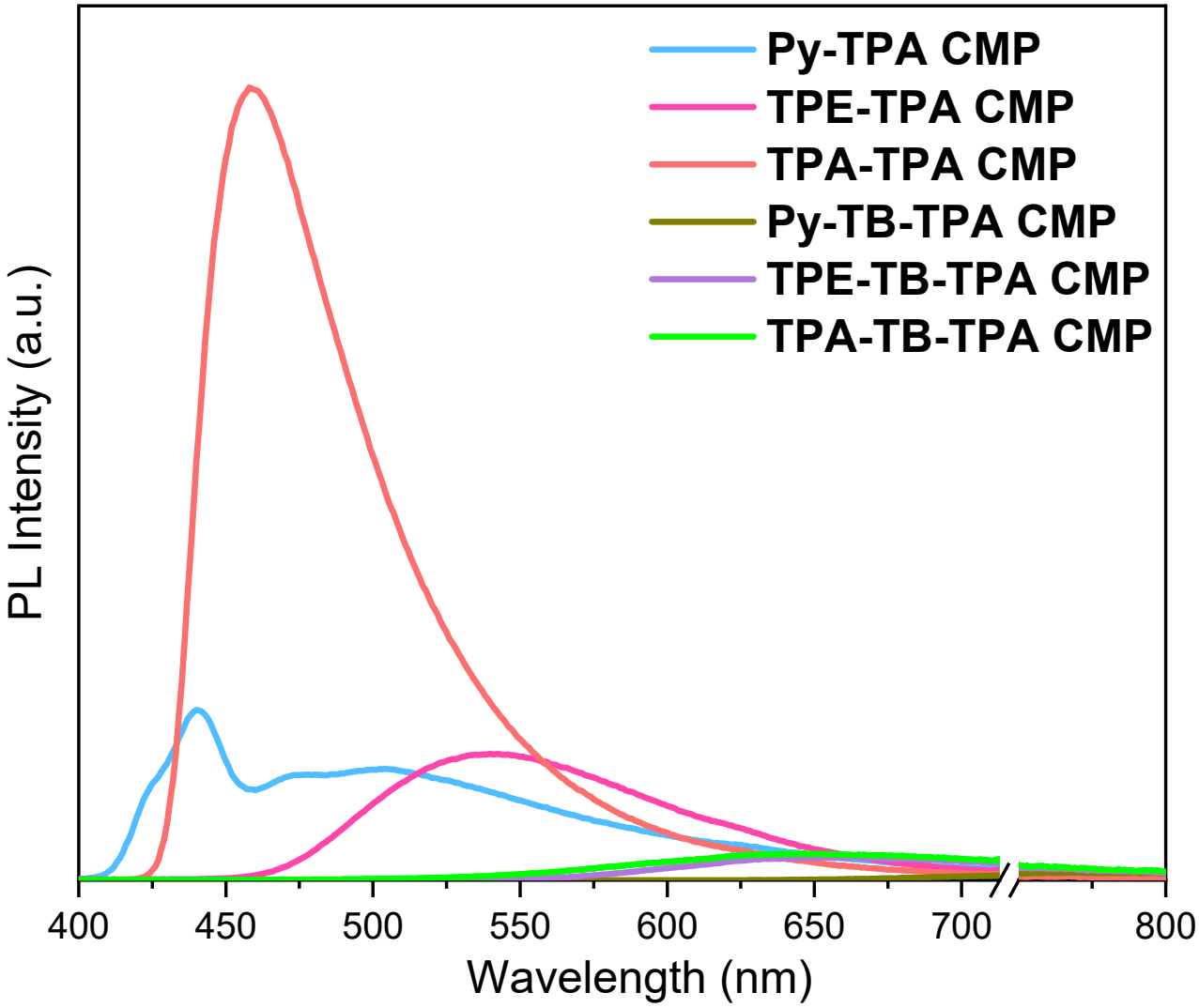

Figure S35. PL spectra of Py-TPA CMP, TPE-TPA CMP, TPA-TPA CMP, Py-TB-TPA CMP, TPE-TB-TPA CMP, and TPA-TB-TPA CMP.

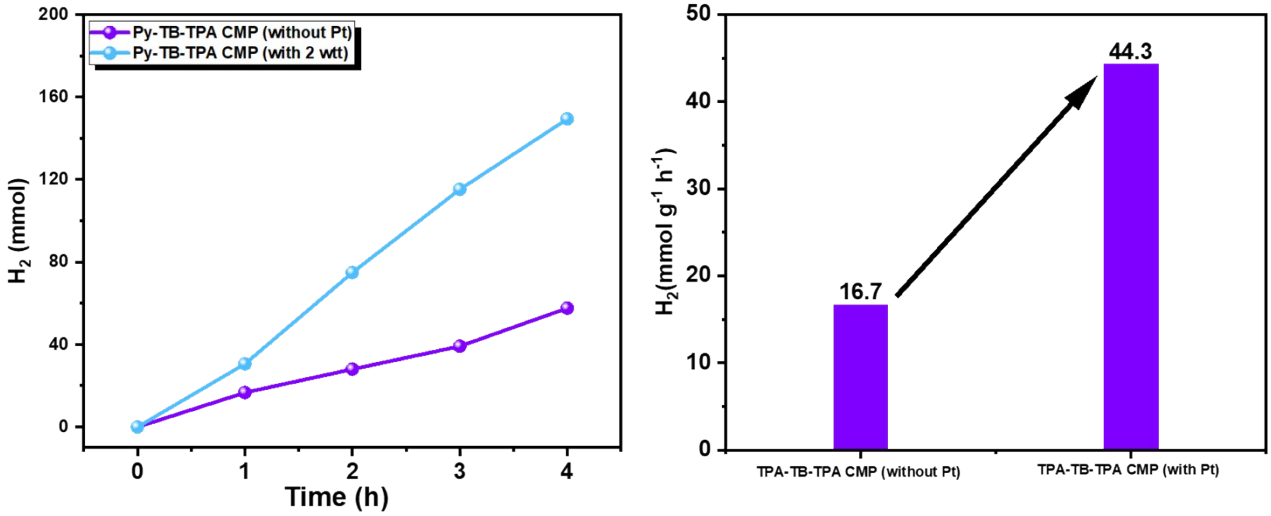

Figure S36. HER data of Py-TB-TPA CMP in the presence and absence of Pt.

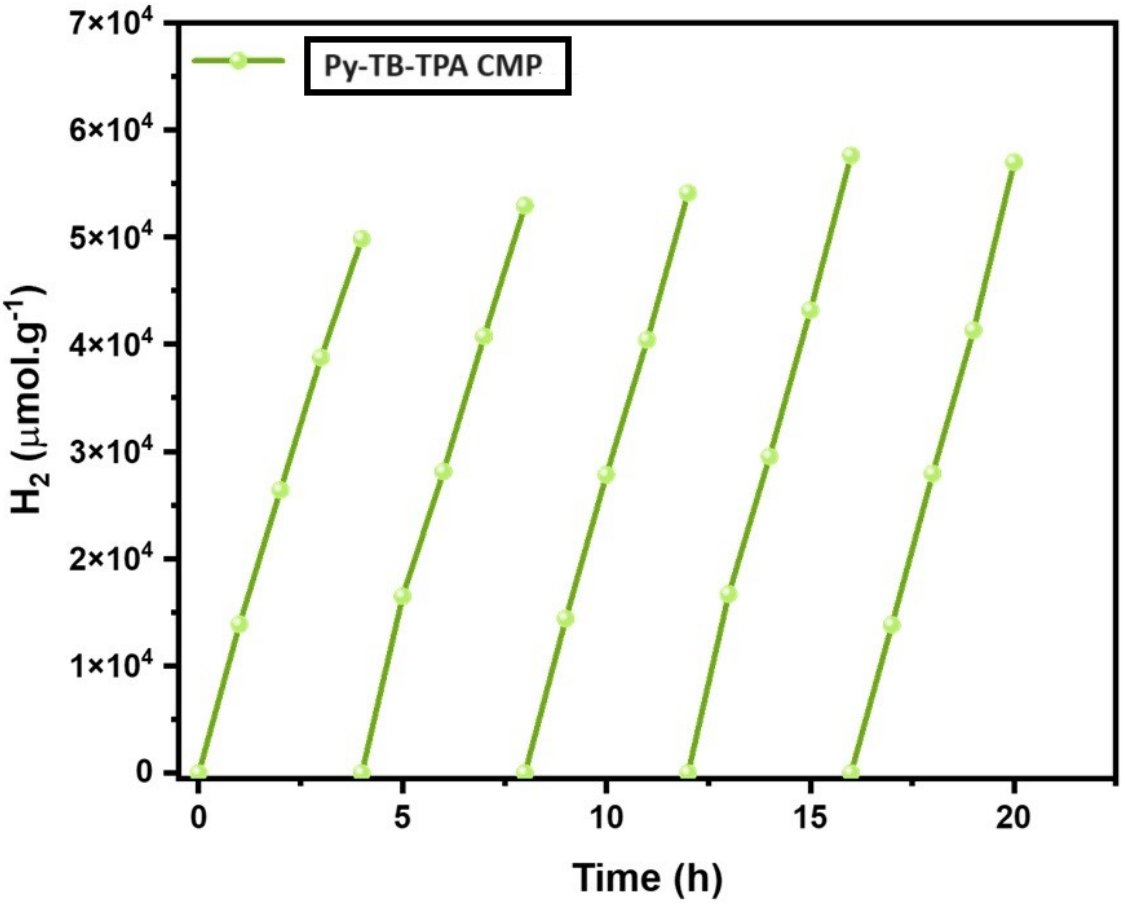

Figure S37. Stability and reusability test using Py-TB-TPA CMP as a photocatalyst under visible-light irradiation.

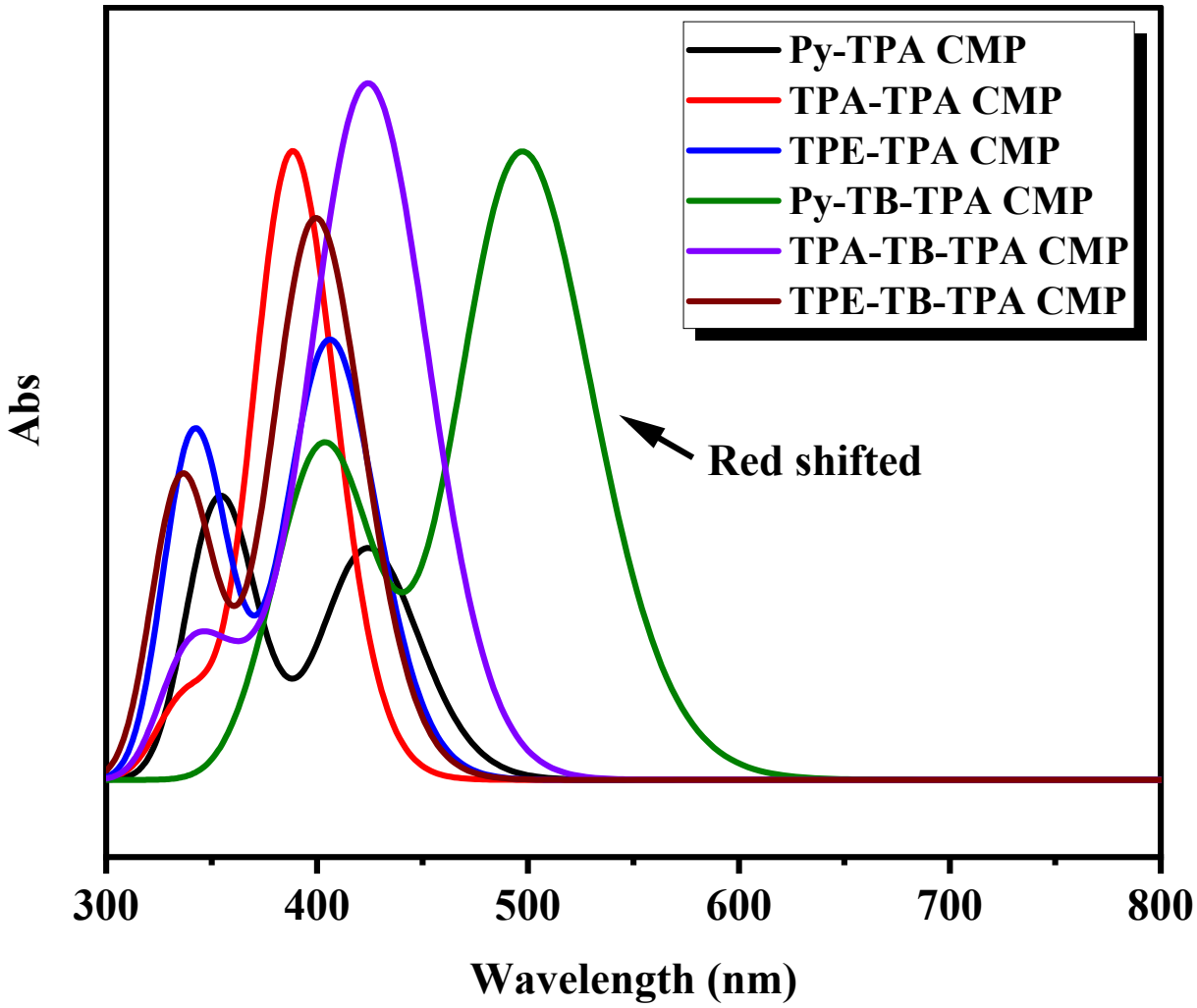

Figure S38. Simulated UV-visible absorption spectra of the studied molecules.

Table S1. Summarized TGA, BET and HER data of TPA-CMPs.

Sample	T_{d5} (°C)	T_{d10} (°C)	Char Yield (wt.%)	Surface Area (m^2/g)	Pore Volume (cm^3/g)	Pore Size (nm)	HER (μmol g^{-1} h^{-1})
TPA-TPA CMP	518	557	72	98	0.22	0.4	44
TPE-TPA CMP	296	357	63	423	0.69	1	119
Py-TPA CMP	387	508	78	913	0.62	1	109
TPA-TB-TPA CMP	370	482	76	459	0.25	1.9	1107
TPE-TB-TPA CMP	376	432	62	487	0.57	1	3633
Py-TB-TPA CMP	306	382	70	454	0.28	1	16700

Table S2. Summarized the ICP-OES results for TPA-TPA CMP, TPE-TPA CMP, Py-TPA CMP, TPA-TB-TPA CMP, TPE-TB-TPA and Py-TB-TPA CMP.

Sample	**Pd (ppm)**
TPA-TPA CMP	8.3
TPE-TPA CMP	5.6
Py-TPA CMP	6.4
TPA-TB-TPA CMP	9
TPE-TB-TPA CMP	4.5
Py-TB-TPA CMP	5.4

Table S3. Summarized the AQY values of Py-TB-TPA CMP at different wavelengths.

	λ = 420 nm	λ = 460 nm	λ = 500 nm	λ = 550 nm	λ = 600 nm
N_A (/mol)	6.022×10^23	6.022×10^23	6.022×10^23	6.022×10^23	6.022×10^23
M (mol)	2.302e-5	1.885e-5	1.987e-5	2.1604e-5	1.157e-5
h (J·s)	6.626×10^-34	6.626×10^-34	6.626×10^-34	6.626×10^-34	6.626×10^-34
c (m/s)	3×10^8	3×10^8	3×10^8	3×10^8	3×10^8
S (m^2)	0.00075	0.00075	0.00075	0.00075	0.00075
P (W/m^2)	22.5	23	25	27	30
t (s)	3600	3600	3600	3600	3600
⌊ (m)	0.00000042	0.00000046	0.0000005	0.00000055	0.0000006
AQY	21.6	15.8	14.1	12.9	5.7

Table S4. Comparative studies of synthesized our synthetic TPA-CMPs and TPA-TB-CMPs with the reported CMPs toward photocatalytic hydrogen evolution.

Photocatalyst	Photocatalytic conditions	Activity (μmol g^{-1} h^{-1})	Reference
Flu-SO Py-SO $FluPh_2$-SO	H_2O/MeOH/TEA, Pt	6060 4940 6840	*Small* **2018**, 14, 1801839
Ta-CMP Ta-CMP-N Ta-CMP-CN	Water/TEOA	48.7 99 698	Macromol. Chem. Phys. 2019, 220, 1900304
PyTA-BC PyTA-BC-Ph	H_2O/MeOH, AA, Pt	5030 2760	*Adv. Opt. Mater.* **2020**, 8, 2000641
TP-BDDA	TEOA/H_2O, Pt	324	J. Am. Chem. Soc. 2018, 140, 1423-1427
Sp^2c-COF Sp^2c-COF_{ERDN}	TEOA/H_2O, Pt	1360 2120	Chem 2019, 5, 1632-1647
NUS-55 NUS-55(Co)	H_2O/Ethanol, TEA	430 2480	Sci. China Chem. 2020, 63, 192-197
TpPa-2	H_2O/ Sodium ascorbate, Ni	1890	Chem. Eng. J. 2020, 379, 122342
PCP4e	Water/MeOH/TEA, Pt	1900	J. Am. Chem. Soc. 2016, 138, 7681-7686
FS-COF	Water/ AA, Pt	16300	Nat. Chem. 2018, 10, 1180-1189
PCP11	Water/MeOH/TEA, Pt	2590	Macromolecules 2016, 49, 6903-6909
DBTD-CMP1	Water/TEOA, Pt	4600	ACS Catal. 2018, 8, 8590-8596
PyBT-2	Water/TEOA, Pt	1060	Appl. Catal. B: Environ. 2018, 228, 1-9
P28	Water/MeOH/TEA	960	Chem. Mater. 2018, 30, 5733-5742
P10	Water/MeOH/TEA	3260	Nat. Commun. 2018, 9, 1-11
S-CMP3	Water/MeOH/TEA, Pt	3110	Chem. Mater. 2019, 31, 305-313
N-PDBT-O	Water/ TEOA	12200	Rapid Commun. 2019, 40, 1800494
P64	Water/MeOH/TEA	3530	J. Am. Chem. Soc. 2019, 141, 9063-9071

MoS_2/PyP(IM)	Water/MeOH	520	Appl. Catal. B: Environ. 2019, 251, 102-111
PSO-FS	Water/TEOA	3400	Angew. Chem. Int. Ed. 2019, 58, 10236-10240
N-CMP (4-CzPN)	Water/TEOA, Pt	2100	Appl. Catal. B: Environ. 2019, 245, 114-121
B-SOBT-1,3,5-E	Water/TEOA	1400	J. Mater. Chem. A 2021, 9,10208-10216
BBT-FC8O5	Water/TEOA	10360	Appl. Surf. Sci. 2020, 499, 143865
Flu-DFBZ	Water/TEOA	14850	Appl. Catal. B: Environ. 2020, 267, 118577
H-CN	Water/TEOA, Pt	4300	J. Colloid Interface Sci. 2021, 581, 159-166
TPET-TTh CMP PyT-TTh CMP	Water/MeOH/AA, Pt Water/MeOH/AA, Pt	4600 18533	Giant, 2024, 17, 100217
TPA-TPA CMP TPE-TPA CMP Py-TPA CMP TPA-TB-TPA CMP TPE-TB-TPA CMP Py-TB-TPA CMP	Water/MeOH/AA Water/MeOH/AA Water/MeOH/AA Water/MeOH/AA Water/MeOH/AA Water/MeOH/AA	44 119 109 1107 3633 16700	This work

Table S5. The calculated MOs energies, energy gap, and global reactivity descriptors of the studied TPA-CMP materials

Quantum descriptors	Py-TPA CMP	TPA-TPA CMP	TPE-TPA CMP	TPA-TB-TPA CMP	TPA-TB-TPA CMP	TPE-TB-TPA CMP
E_{HOMO} (eV)	-5.00	-4.76	-4.95	**-4.91**	-4.85	-5.04
E_{LUMO} (eV)	-1.70	-1.06	-1.48	**-2.07**	-1.52	-1.51
ΔE (eV)	3.30	3.70	3.47	**2.84**	3.32	3.53
Electron affinity *A* (eV)	1.70	1.06	1.48	**2.07**	1.52	1.51
Ionization potential I (eV)	5.00	4.76	4.95	**4.91**	4.85	5.04
Chemical hardness η (eV)	1.65	1.85	1.73	**1.42**	1.66	1.77
Softness S (eV^{-1})	0.30	0.27	0.29	**0.35**	0.30	0.28
Electronegativity χ (eV)	3.35	2.91	3.22	**3.49**	3.18	3.27
Electrophilicity index ω (eV)	3.40	2.29	2.98	**4.29**	3.05	3.04